TABLE II. Significantly Upregulated Genes in Cells Grown on $CaCl_2$-Treated Titanium Disks (Top 30)

Symbol	Entrez Gene Name	Fold Change
SPP1 (OPN)	Secreted phosphoprotein 1	6.252
PRSS1/PRSS3	Protease, serine, 1 (trypsin 1)	4.009
MMP13	Matrix metallopeptidase 13 (collagenase 3)	3.882
GPR56	G protein-coupled receptor 56	3.640
C13orf15	Regulator of cell cycle	3.578
IGFBP1	Insulin-like growth factor binding protein 1	3.540
PTGS1	Prostaglandin-endoperoxide synthase 1 (prostaglandin G/H synthase and cyclooxygenase)	3.500
TFPI2	Tissue factor pathway inhibitor 2	3.406
YTHDC1	YTH domain containing 1	3.371
CENPM	Centromere protein M	3.235
COL15A1	Collagen, type XV, alpha 1	3.174
AQP1	Aquaporin 1 (Colton blood group)	3.149
RPL18A	Ribosomal protein L18a	3.098
DUSP4	Dual specificity phosphatase 4	3.095
DIXDC1	DIX domain containing 1	3.016
TMEM158	Transmembrane protein 158 (gene/pseudogene)	2.791
C16orf57	Chromosome 16 open reading frame 57	2.787
SMC1A	Structural maintenance of chromosomes 1A	2.761
ARID5B	AT rich interactive domain 5B (MRF1-like)	2.655
TNFSF10	Tumor necrosis factor (ligand) superfamily, member 10	2.648
IL17RC	Interleukin 17 receptor C	2.624
DCTN4	Dynactin 4 (p62)	2.605
ING3	Inhibitor of growth family, member 3	2.557
NOL6	Nucleolar protein family 6 (RNA-associated)	2.555
PLTP	Phospholipid transfer protein	2.555
SLC29A1	Solute carrier family 29 (nucleoside transporters), member 1	2.507
MCM5	Minichromosome maintenance complex component 5	2.502
ENPP1	Ectonucleotide pyrophosphatase/phosphodiesterase 1	2.497
ADAMTS16	ADAM metallopeptidase with thrombospondin type 1 motif, 16	2.493
SMURF1	SMAD specific E3 ubiquitin protein ligase 1	2.491

TABLE III. Significantly Upregulated Genes in Cells Grown on $Ca(OH)_2$-Treated Titanium Disks (Top 30)

Symbol	Entrez Gene Name	Fold Change
SPP1 (OPN)	Secreted phosphoprotein 1	17.721
MMP13	Matrix metallopeptidase 13 (collagenase 3)	16.725
RGS2	Regulator of G-protein signaling 2, 24kDa	8.677
TFPI2	Tissue factor pathway inhibitor 2	7.763
PTGS1	Prostaglandin-endoperoxide synthase 1 (prostaglandin G/H synthase and cyclooxygenase)	7.343
SLC16A6	Solute carrier family 16, member 6 (monocarboxylic acid transporter 7)	7.286
IGFBP1	Insulin-like growth factor binding protein 1	6.677
DUSP4	Dual specificity phosphatase 4	6.649
PCDH19	Protocadherin 19	5.943
PTHLH	Parathyroid hormone-like hormone	5.630
GPR56	G protein-coupled receptor 56	5.129
SLC29A1	Solute carrier family 29 (nucleoside transporters), member 1	4.924
C13orf15	Regulator of cell cycle	4.750
ENPP1	Ectonucleotide pyrophosphatase/phosphodiesterase 1	4.717
EREG	Epiregulin	4.712
TNFSF10	Tumor necrosis factor (ligand) superfamily, member 10	4.436
CXCL6	Chemokine (C-X-C motif) ligand 6 (granulocyte chemotactic protein 2)	4.404
TMEM158	Transmembrane protein 158 (gene/pseudogene)	4.403
PRSS1/PRSS3	Protease, serine, 1 (trypsin 1)	4.397
BMP2	Bone morphogenetic protein 2	4.140
COL10A1	Collagen, type X, alpha 1	3.739
FOXQ1	Forkhead box Q1	3.670
MGP	Matrix Gla protein	3.488
PLAU	Plasminogen activator, urokinase	3.364
CENPM	Centromere protein M	3.288
IL6R	Interleukin 6 receptor	3.223
ITGA2	Integrin, alpha 2 (CD49B, alpha 2 subunit of VLA-2 receptor)	3.205
CLU	Clusterin	3.163
FPR1	Formyl peptide receptor 1	3.114
ESCO2	Establishment of cohesion 1 homolog 2 (*S. cerevisiae*)	3.084

TABLE IV. Significantly Upregulated Genes Associated with *'Formation of Bone'* on $Ca(OH)_2$-Treated Titanium Disks vs. $CaCl_2$-Trated Disks

Symbol	Entrez Gene Name	Fold Change
SPP1 (OPN)	Secreted phosphoprotein 1 (Osteopontin)	2.835
PTHLH	Parathyroid hormone-like hormone	2.308
FGF1	Fibroblast growth factor 1 (acidic)	2.202
BMP2	Bone morphogenetic protein 2	2.175
PTGS1	Prostaglandin-endoperoxide synthase 1 (prostaglandin G/H synthase and cyclooxygenase 1)	2.098
PTGS2	Prostaglandin-endoperoxide synthase 2 (prostaglandin G/H synthase and cyclooxygenase 2)	2.008

These genes significantly overlapped with the genes associated with "formation of bone" by IPA ($p = 3.96 \times 10^{-4}$).

mesenchymal progenitor cells.[44] BMP2 induces Cox2 in osteoblasts[45] and in mesenchymal cells.[46] It was also reported that extracellular calcium increases expression of BMP2.[47,48] Furthermore, the calcium–calcineurin–nuclear factor of activated T-cell signaling pathway has an important role in the PTH induction of Cox2.[49] Taken together, our results suggest that $Ca(OH)_2$ treatment of titanium disks induces osteogenic differentiation in hMSCs via induction of BMP2, Cox2, and PTHLH. In contrast, Smad signaling was downregulated by chemically modified titanium surfaces (Figs. 5–7). A previous study demonstrated that noncanonical BMP signaling regulates Cox2 transcription.[46] These observations suggest noncanonical BMP signaling (independent of Smad signaling) might mediate the osteogenic differentiation of hMSCs on $Ca(OH)_2$-treated titanium.

Postanalysis of microarray data was performed by IPA. NaOH treatment induced the osteogenic promoter WNT and its cell surface receptor Frizzled, as well as Axin and APC,

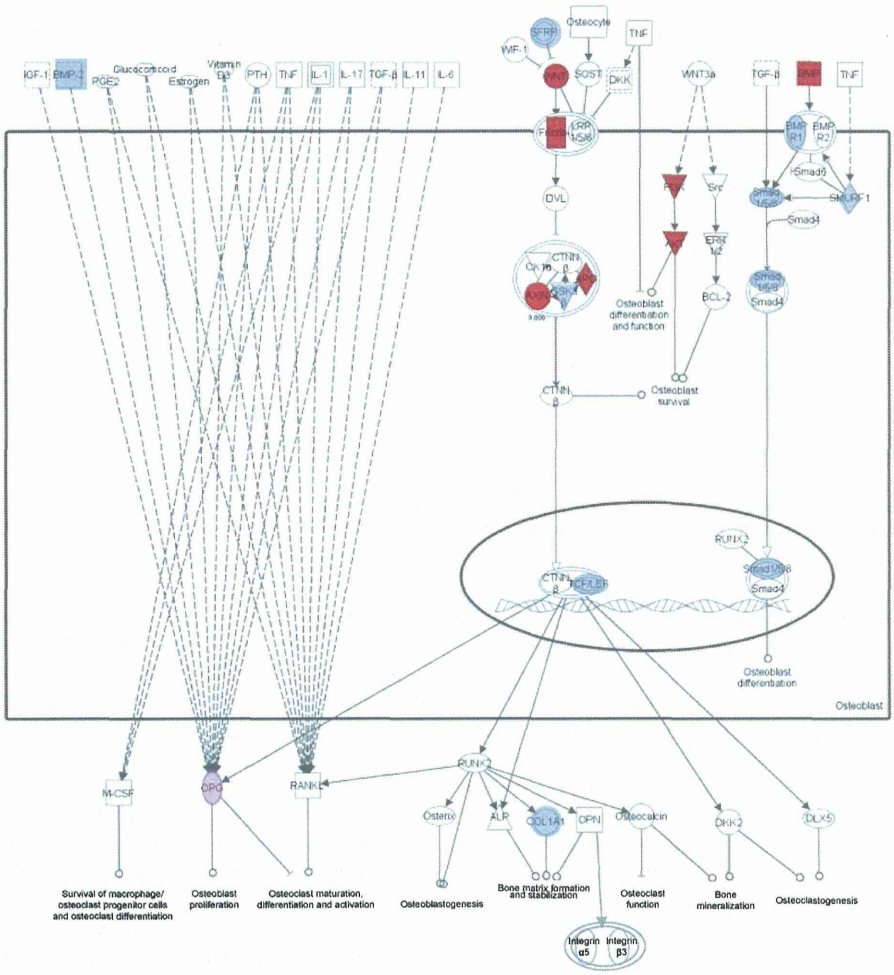

FIGURE 5. Differentially expressed genes in the canonical pathway in osteoblasts were significantly changed by NaOH treatment versus untreated conditions. Upregulated (more than twice), downregulated (less than 1/2), induced, and suppressed genes are indicated in pink, green, red, and light blue, respectively.

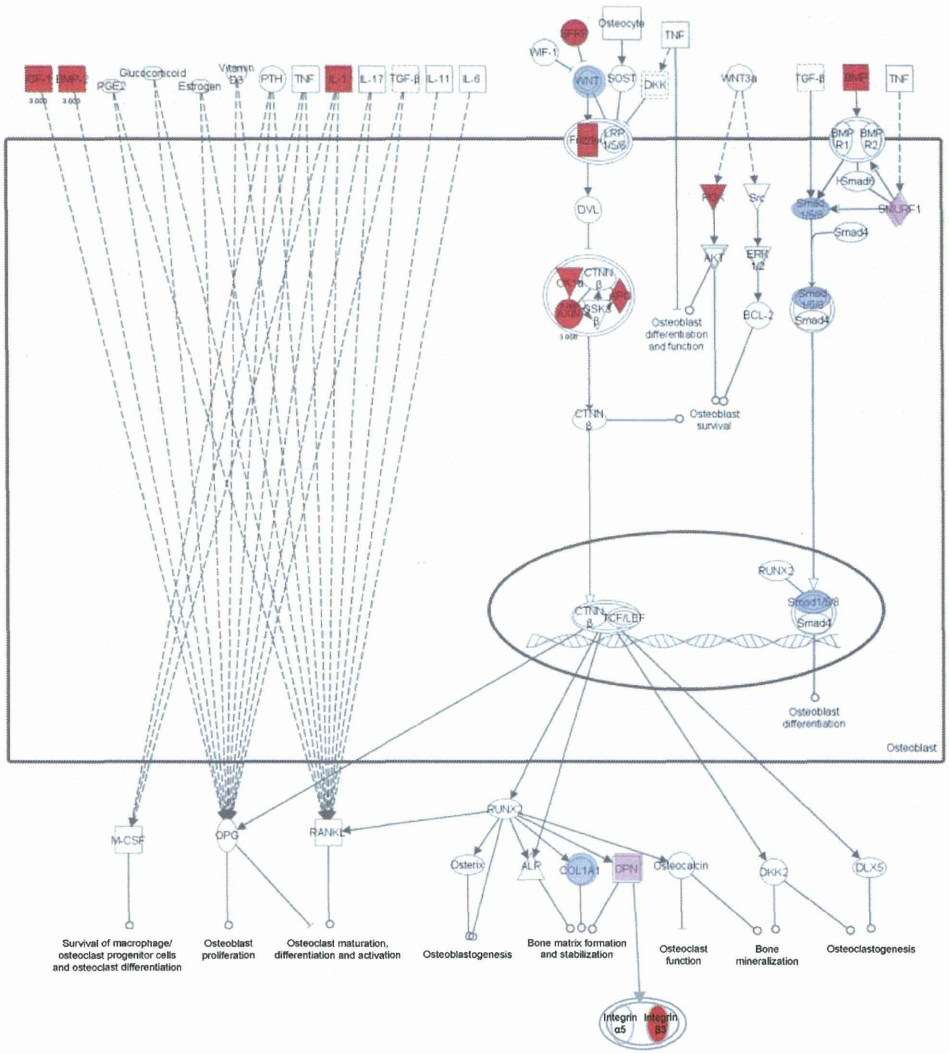

FIGURE 6. Differentially expressed genes in the canonical osteoblast pathway on $CaCl_2$-treated disks versus untreated disks. Upregulated (more than twice), downregulated (less than 1/2), induced, and suppressed genes are indicated in pink, green, red, and light blue, respectively.

scaffolding proteins that bind to intracellular Wnt/β-catenin signaling molecules. RANKL decoy receptor OPG expression was upregulated by NaOH (Fig. 5). $CaCl_2$ treatment induced expression of Frizzled, Axin, and APC as well as of the osteogenic markers BMP and IGF-1. The bone matrix protein OPN was upregulated, and the expression of integrin β3 was induced following OPN upregulation by $CaCl_2$ (Fig. 6). $Ca(OH)_2$ treatment induced LRP5/6 and essential coreceptors of Wnt ligands for canonical β-catenin-dependent signal transduction, in addition to WNT, Frizzled, Axin, and APC. BMP, IGF-1, and integrin β3 were also induced by $Ca(OH)_2$. In addition to OPN, OCN was upregulated by $Ca(OH)_2$ (Fig. 7).

Wnt/β-catenin signaling in mesenchymal progenitors controls osteoblast differentiation[50]; surface properties of titanium regulate stem cell fate and induce osteoblast differentiation via the Wnt calcium-dependent pathway and Wnt5a enhanced osteogenesis through positive feedback with integrins.[51] Previous studies have shown the integrin family plays a major role in osteoblastic differentiation on variously modified titanium surfaces.[4,5,10,14] We observed that calcium modification of the titanium surface induced integrin β3 following OPN upregulation. Wnt/β-catenin signaling in hMSCs was also promoted by the calcium modification, more by $Ca(OH)_2$ than $CaCl_2$ treatment. These observations suggest that calcium modification of titanium surfaces induces osteogenic differentiation in hMSCs in the absence of osteogenic factors by activation of Wnt/β-catenin signaling.

In this study, $Ca(OH)_2$ treatment of titanium surface was more effective to osteogenic differentiation in hMSC than $CaCl_2$ treatment, this might be caused by the difference of the amount of calcium ions and apatite formation on the titanium surface between the two kinds of calcium treatments. We

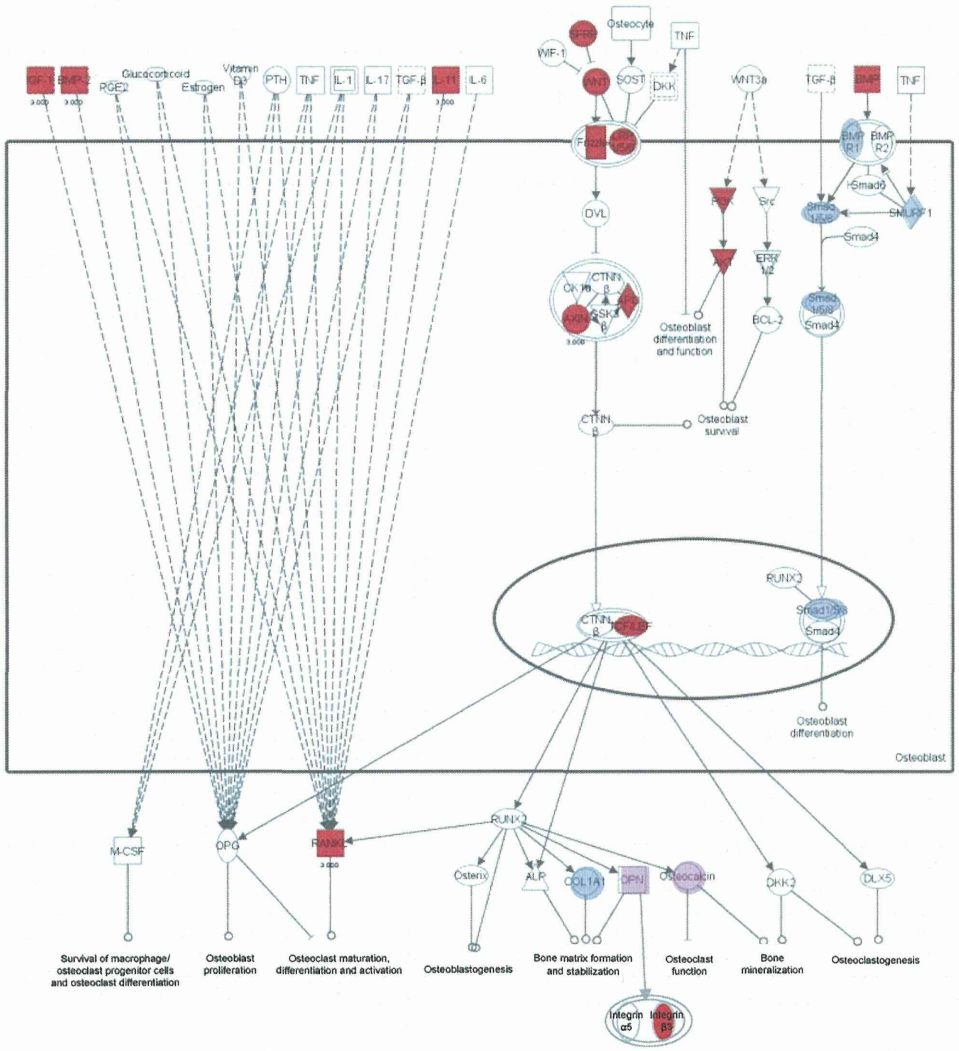

FIGURE 7. Differentially expressed genes in the canonical osteoblast pathway on $Ca(OH)_2$ versus untreated disks. Upregulated (more than twice), downregulated (less than 1/2), induced, and suppressed genes are indicated in pink, green, red, and light blue, respectively.

suggested that $Ca(OH)_2$ treatment of titanium disks induced osteogenic differentiation in hMSCs by the upregulation of BMP2, Cox2, and PTHLH compared with $CaCl_2$ treatment, and the activation of Wnt/β-catenin signaling.

CONCLUSIONS

In this study, we chemically modified titanium surfaces with $CaCl_2$ or $Ca(OH)_2$ after NaOH treatment to alter the surface topology and incorporate calcium ions; subsequently, we investigated the influence of these treatments on osteogenic differentiation in hMSCs in the absence of osteogenic supplements. Calcium modification by $CaCl_2$ or $Ca(OH)_2$ affects cell morphology and molecular responses in hMSCs. Whole genome expression analysis suggested that calcium modification of the titanium surface activates Wnt/β-catenin signaling. In addition, $Ca(OH)_2$ treatment upregulated expression of BMP2, Cox2, and PTHLH. $Ca(OH)_2$ treatment induces osteogenic differentiation in hMSCs, whereas $CaCl_2$ has a limited effect; this may depend on whether there are significant differences between treatments with respect to the amount of calcium ions and apatite formation on the titanium surface.

ACKNOWLEDGMENTS

This work was supported by the Health and Labour Sciences Research Grants for Research on Regulatory Science of Pharmaceuticals and Medical Devices (H22-IYAKU-IPPAN-009, H24- IYAKU-SHITEI-018) from the Ministry of Health, Labour and Welfare of Japan.

REFERENCES

1. Walivaara B, Aronsson BO, Rodahl M, Lausmaa J, Tengvall P. Titanium with different oxides: In vitro studies of protein adsorption and contact activation. Biomaterials 1994;15:827–834.

2. Rupp F, Axmann D, Ziegler C, Geis-Gerstorfer J. Adsorption/desorption phenomena on pure and Teflon AF-coated titania surfaces studied by dynamic contact angle analysis. J Biomed Mater Res 2002;62:567–578.
3. Sousa SR, Lamghari M, Sampaio P, Moradas-Ferreira P, Barbosa MA. Osteoblast adhesion and morphology on TiO_2 depends on the competitive preadsorption of albumin and fibronectin. J Biomed Mater Res A 2008;84:281–290.
4. Anselme K. Osteoblast adhesion on biomaterials. Biomaterials 2000;21:667–681.
5. Lavenus S, Berreur M, Trichet V, Pilet P, Louarn G, Layrolle P. Adhesion and osteogenic differentiation of human mesenchymal stem cells on titanium nanopores. Eur Cell Mater 2011;22:84–96; discussion 96.
6. Hu Y, Cai K, Luo Z, Zhang Y, Li L, Lai M, Hou Y, Huang Y, Li J, Ding X, Zhang B, Sung KL. Regulation of the differentiation of mesenchymal stem cells in vitro and osteogenesis in vivo by microenvironmental modification of titanium alloy surfaces. Biomaterials 2012;33:3515–3528.
7. Vlacic-Zischke J, Hamlet SM, Friis T, Tonetti MS, Ivanovski S. The influence of surface microroughness and hydrophilicity of titanium on the up-regulation of TGFbeta/BMP signalling in osteoblasts. Biomaterials 2011;32:665–671.
8. Khang D, Choi J, Im YM, Kim YJ, Jang JH, Kang SS, Nam TH, Song J, Park JW. Role of subnano-, nano- and submicron-surface features on osteoblast differentiation of bone marrow mesenchymal stem cells. Biomaterials 2012;33:5997–6007.
9. Gittens RA, McLachlan T, Olivares-Navarrete R, Cai Y, Berner S, Tannenbaum R, Schwartz Z, Sandhage KH, Boyan BD. The effects of combined micron-/submicron-scale surface roughness and nanoscale features on cell proliferation and differentiation. Biomaterials 2011;32:3395–3403.
10. Olivares-Navarrete R, Raz P, Zhao G, Chen J, Wieland M, Cochran DL, Chaudhri RA, Ornoy A, Boyan BD, Schwartz Z. Integrin alpha2beta1 plays a critical role in osteoblast response to micron-scale surface structure and surface energy of titanium substrates. Proc Natl Acad Sci USA 2008;105:15767–15772.
11. Wennerberg A, Albrektsson T. Effects of titanium surface topography on bone integration: A systematic review. Clin Oral Implants Res 2009;20(Suppl 4):172–184.
12. Schwartz Z, Nasazky E, Boyan BD. Surface microtopography regulates osteointegration: The role of implant surface microtopography in osteointegration. Alpha Omegan 2005;98:9–19.
13. Park JH, Olivares-Navarrete R, Wasilewski CE, Boyan BD, Tannenbaum R, Schwartz Z. Use of polyelectrolyte thin films to modulate osteoblast response to microstructured titanium surfaces. Biomaterials 2012;33:5267–5277.
14. Wang L, Zhao G, Olivares-Navarrete R, Bell BF, Wieland M, Cochran DL, Schwartz Z, Boyan BD. Integrin beta1 silencing in osteoblasts alters substrate-dependent responses to 1,25-dihydroxy vitamin D3. Biomaterials 2006;27:3716–3725.
15. Guo J, Padilla RJ, Ambrose W, De Kok IJ, Cooper LF. The effect of hydrofluoric acid treatment of TiO2 grit blasted titanium implants on adherent osteoblast gene expression in vitro and in vivo. Biomaterials 2007;28:5418–5425.
16. Mendonca G, Mendonca DB, Simoes LG, Araujo AL, Leite ER, Duarte WR, Aragao FJ, Cooper LF. The effects of implant surface nanoscale features on osteoblast-specific gene expression. Biomaterials 2009;30:4053–4062.
17. Mendonca G, Mendonca DB, Aragao FJ, Cooper LF. The combination of micron and nanotopography by H_2SO_4/H_2O_2 treatment and its effects on osteoblast-specific gene expression of hMSCs. J Biomed Mater Res A 2010;94:169–179.
18. Kim HM, Miyaji F, Kokubo T, Nakamura T. Preparation of bioactive Ti and its alloys via simple chemical surface treatment. J Biomed Mater Res 1996;32:409–417.
19. Yan WQ, Nakamura T, Kobayashi M, Kim HM, Miyaji F, Kokubo T. Bonding of chemically treated titanium implants to bone. J Biomed Mater Res 1997;37:267–275.
20. Kim HM, Miyaji F, Kokubo T, Nishiguchi S, Nakamura T. Graded surface structure of bioactive titanium prepared by chemical treatment. J Biomed Mater Res 1999;45:100–107.
21. Takadama H, Kim HM, Kokubo T, Nakamura T. TEM-EDX study of mechanism of bonelike apatite formation on bioactive titanium metal in simulated body fluid. J Biomed Mater Res 2001;57: 441–448.
22. Nishiguchi S, Kato H, Neo M, Oka M, Kim HM, Kokubo T, Nakamura T. Alkali- and heat-treated porous titanium for orthopedic implants. J Biomed Mater Res 2001;54:198–208.
23. Fujibayashi S, Neo M, Kim HM, Kokubo T, Nakamura T. Osteoinduction of porous bioactive titanium metal. Biomaterials 2004;25: 443–450.
24. Takemoto M, Fujibayashi S, Neo M, Suzuki J, Kokubo T, Nakamura T. Mechanical properties and osteoconductivity of porous bioactive titanium. Biomaterials 2005;26:6014–6023.
25. Cooper LF, Zhou Y, Takebe J, Guo J, Abron A, Holmen A, Ellingsen JE. Fluoride modification effects on osteoblast behavior and bone formation at TiO2 grit-blasted c.p. titanium endosseous implants. Biomaterials 2006;27:926–936.
26. Kizuki T, Takadama H, Matsushita T, Nakamura T, Kokubo T. Preparation of bioactive Ti metal surface enriched with calcium ions by chemical treatment. Acta Biomater 2010;6:2836–2842.
27. Jiang Y, Jahagirdar BN, Reinhardt RL, Schwartz RE, Keene CD, Ortiz-Gonzalez XR, Reyes M, Lenvik T, Lund T, Blackstad M, Du J, Aldrich S, Lisberg A, Low WC, Largaespada DA, Verfaillie CM. Pluripotency of mesenchymal stem cells derived from adult marrow. Nature 2002;418:41–49.
28. Rosenthal N. Prometheus's vulture and the stem-cell promise. N Engl J Med 2003;349:267–274.
29. Korbling M, Estrov Z. Adult stem cells for tissue repair—A new therapeutic concept? N Engl J Med 2003;349:570–582.
30. Hishikawa K, Miura S, Marumo T, Yoshioka H, Mori Y, Takato T, Fujita T. Gene expression profile of human mesenchymal stem cells during osteogenesis in three-dimensional thermoreversible gelation polymer. Biochem Biophys Res Commun 2004;317: 1103–1107.
31. Horwitz EM, Gordon PL, Koo WK, Marx JC, Neel MD, McNall RY, Muul L, Hofmann T. Isolated allogeneic bone marrow-derived mesenchymal cells engraft and stimulate growth in children with osteogenesis imperfecta: Implications for cell therapy of bone. Proc Natl Acad Sci USA 2002;99:8932–8937.
32. Mangi AA, Noiseux N, Kong D, He H, Rezvani M, Ingwall JS, Dzau VJ. Mesenchymal stem cells modified with Akt prevent remodeling and restore performance of infarcted hearts. Nat Med 2003;9: 1195–1201.
33. Strauer BE, Brehm M, Zeus T, Kostering M, Hernandez A, Sorg RV, Kogler G, Wernet P. Repair of infarcted myocardium by autologous intracoronary mononuclear bone marrow cell transplantation in humans. Circulation 2002;106:1913–1918.
34. Petersen BE, Bowen WC, Patrene KD, Mars WM, Sullivan AK, Murase N, Boggs SS, Greenberger JS, Goff JP. Bone marrow as a potential source of hepatic oval cells. Science 1999;284: 1168–1170.
35. Behonick DJ, Xing Z, Lieu S, Buckley JM, Lotz JC, Marcucio RS, Werb Z, Miclau T, Colnot C. Role of matrix metalloproteinase 13 in both endochondral and intramembranous ossification during skeletal regeneration. PLoS One 2007;2:e1150.
36. Dvorak-Ewell MM, Chen TH, Liang N, Garvey C, Liu B, Tu C, Chang W, Bikle DD, Shoback DM. Osteoblast extracellular Ca^{2+}-sensing receptor regulates bone development, mineralization, and turnover. J Bone Miner Res 2011;26:2935–2947.
37. Albrektsson T, Wennerberg A. Oral implant surfaces: Part 1—Review focusing on topographic and chemical properties of different surfaces and in vivo responses to them. Int J Prosthodont 2004;17:536–543.
38. Albrektsson T, Wennerberg A. Oral implant surfaces: Part 2—Review focusing on clinical knowledge of different surfaces. Int J Prosthodont 2004;17:544–564.
39. McBeath R, Pirone DM, Nelson CM, Bhadriraju K, Chen CS. Cell shape, cytoskeletal tension, and RhoA regulate stem cell lineage commitment. Dev Cell 2004;6:483–495.
40. Rodriguez JP, Gonzalez M, Rios S, Cambiazo V. Cytoskeletal organization of human mesenchymal stem cells (MSC) changes during their osteogenic differentiation. J Cell Biochem 2004;93:721–731.
41. Kumar G, Tison CK, Chatterjee K, Pine PS, McDaniel JH, Salit ML, Young MF, Simon CG Jr. The determination of stem cell fate by 3D scaffold structures through the control of cell shape. Biomaterials 2011;32:9188–9196.

42. Kumar G, Waters MS, Farooque TM, Young MF, Simon CG Jr. Freeform fabricated scaffolds with roughened struts that enhance both stem cell proliferation and differentiation by controlling cell shape. Biomaterials 2012;33:4022–4030.
43. Simon AM, Manigrasso MB, O'Connor JP. Cyclo-oxygenase 2 function is essential for bone fracture healing. J Bone Miner Res 2002;17:963–976.
44. Lee HW, Kim SY, Kim AY, Lee EJ, Choi J-Y, Kim JB. Adiponection stimulates osteoblast differntiation through induction of COX2 in mesenchymal progenitor cells. Stem Cells 2009;27: 2254–2262.
45. Chikazu D, Li X, Kawaguchi H, Sakuma Y, Voznesensky OS, Adams DJ, Xu M, Hoshi K, Katavic V, Herschman HR, Raisz L, Pilbeam CC. Bone morphogenetic protein 2 induces cyclo-oxygenase 2 in osteoblasts via Cbfa1 binding site: Role in effects of bone mprphogenetic protein 2 in vitro and in vivo. J Bone Miner Res 2002;17:1430–1440.
46. Susperregui ARG, Gamell C, Rodíguez-Carballo E, Ortuño MJ, Bartrons R, Rosa JL, Ventura F. Noncanonical BMP signaling regulates *Cyclooxygenase-2* transcription. Mol Endocrinol 2011;25: 1006–1017.
47. Peiris D, Pacheco I, Spencer C, MacLeod RJ. The extracellular calcium-sensing receptor reciprocally regulates the secretion of BMP-2 and the BMP antagonist Noggin in colonic myofibroblasts. Am J Physiol Gastrointest Liver Physiol 2007;292:G753–G766.
48. Tada H, Nemoto E, Kanaya S, Hamaji N, Sato H, Shimauchi H. Elevated extracellular calcium increases expression of bone morphogenetic protein-2 gene via a calcium channel and ERK pathway in human dental pulp cells. Biochem Biophys Res Commun 2010;394:1093–1097.
49. Huang H, Chikazu D, Voznesensky OS, Herschman HR, Kream BE, Drissi H, Pilbeam CC. Parathyroid hormone induction of cycloxygenase-2 in murine osteoblasts: Role of the calcium–calcineurin–NFAT pathway. J Bone Miner Res 2010;25:819–829.
50. Day TF, Guo X, Garrett-Beal L, Yang Y. Wnt/beta-catenin signaling in mesenchymal progenitors controls osteoblast and chondrocyte differentiation during vertebrate skeletogenesis. Dev Cell 2005;8: 739–750.
51. Olivares-Navarrete R, Hyzy SL, Park JH, Dunn GR, Haithcock DA, Wasilewski CE, Boyan BD, Schwartz Z. Mediation of osteogenic differentiation of human mesenchymal stem cells on titanium surfaces by a Wnt-integrin feedback loop. Biomaterials 2011;32:6399–6411.

Society For Biomaterials

A development and biological safety evaluation of novel PVC medical devices with surface structures modified by UV irradiation to suppress plasticizer migration

Yuji Haishima,[1] Kazuo Isama,[2] Chie Hasegawa,[1] Toshiyasu Yuba,[3] Atsuko Matsuoka[1]

[1]Division of Medical Devices, National Institute of Health Sciences, 1-18-1 Kamiyoga, Setagaya-ku, Tokyo 158-8501, Japan
[2]Division of Environmental Chemistry, National Institute of Health Sciences, 1-18-1 Kamiyoga, Setagaya-ku, Tokyo 158-8501, Japan
[3]Customer Technical Center, Kawasumi Laboratories, INC., 1-12 Minami Watarida, Kawasaki-ku, Kawasaki City, Kanagawa 210-0855, Japan

Received 30 May 2012; revised 15 October 2012; accepted 4 December 2012
Published online 15 February 2013 in Wiley Online Library (wileyonlinelibrary.com). DOI: 10.1002/jbm.a.34558

Abstract: This study examines the chemical, physicochemical, and biological properties of PVC sheets treated with UV irradiation on their surfaces to suppress the elution of a plasticizer, di-(2-ethylhexyl) phthalate (DEHP), for developing novel polyvinyl chloride (PVC) medical devices. The PVC sheets irradiated under conditions 1 (52.5 $\mu W/cm^2$, 136 J/cm^2) and 2 (0.45 mW/cm^2, 972 J/cm^2) exhibited considerable toxicity in cytotoxicity tests and chromosome aberration tests due to the generation of DEHP oxidants, but no toxicity was detected in the PVC sheet irradiated under condition 3 (8.3 mW/cm^2, 134 J/cm^2). The release of DEHP from the surface irradiated under condition 3 was significantly suppressed, and mono-(2-ethylhexyl) phthalate (MEHP) converted from a portion of DEHP could be easily removed from the surface by washing with methanol. The physicochemical properties of the surface regarding the suppression of DEHP elution remained stable through all sterilizations tested, but MEHP elution was partially recrudesced by the sterilizations except for gamma irradiation. These results indicated that UV irradiation using a strong UV-source over a short time (condition 3) followed by methanol washing and gamma sterilization may be useful for preparing novel PVC products that did not elute plasticizers and do not exhibit toxicity originating from UV irradiation. © 2013 Wiley Periodicals, Inc. J Biomed Mater Res Part A: 101A: 2630–2643, 2013.

Key Words: DEHP, MEHP, UV irradiation, surface modification, PVC medical device

How to cite this article: Haishima Y, Isama K, Hasegawa C, Yuba T, Matsuoka A. 2013. A development and biological safety evaluation of novel PVC medical devices with surface structures modified by UV irradiation to suppress plasticizer migration. J Biomed Mater Res Part A 2013:101A:2630–2643.

INTRODUCTION

Phthalate esters, particularly di-(2-ethylhexyl) phthalate (DEHP), have been extensively used as plasticizers due to their ability to increase the flexibility of polyvinyl chloride (PVC), a plastic polymer used in a wide array of products including medical devices such as tubing, intravenous bags, blood containers, and catheters. DEHP is easily eluted from PVC products into foods, pharmaceuticals, and body fluids that touch the plastic, causing the migration of DEHP directly and/or indirectly into the human body.[1,2]

Some phthalates, including DEHP, are considered toxic exhibiting effects in young rodents similar to endocrine disruptors that result in antiandrogenic effects in male rats, altering the development of the male reproductive system and the production of normal sperm.[3–5] It has been indicated that mono-(2-ethylhexyl) phthalate (MEHP) is an active metabolite of DEHP and suggested that any toxic effects of orally ingested DEHP are likely derived from the corresponding monoester, not from the intact DEHP.[6–9] Although the *in vivo* reproductive and developmental toxicity of DEHP on the human body is not yet well understood, recent *in vitro* toxicological studies used human cells have reported that MEHP causes adverse effects such as reduction of the number of germ cells by increasing their apoptosis without altering their proliferation.[10–12] Therefore, precautions should be taken to limit its exposure to humans, particularly high-risk patients such as male neonates, male fetuses, and peripubertal males.

The use of plasticizers other than DEHP is one option for developing safer PVC products for humans use. PVC medical devices that use trioctyl trimellitate or acetyl tributyl citrate instead of DEHP have already been developed. The devices are commercially available, but not popular in the medical field because of reduced performance in comparison with traditional PVC products. The development of other alternate plasticizers is also in progress, particularly in Europe. BASF, a chemical company in Ludwigshafen, Germany, has developed Hexamoll® DINCH, a di-isononyl-

Correspondence to: Y. Haishima; e-mail: haishima@nihs.go.jp

cyclohexane-1,2-dicarboxylate whose biological safety evaluation indicates that it could serve as a substitute for DEHP.[13,14]

The use of devices other than PVC products for medical treatment is another available option. Alternate biomaterials such as polyethylene, polypropylene, polystyrene, polycarbonate, polyurethane, and silicon have been used to produce medical devices such as feeding tubes, filters, catheters, and administration sets containing several tubes. Although some of these are currently commercially available, some has adverse events such as cracks, fractures, solution leakage, or air contamination originating from loose connecters have occurred because of the poor flexibility and durability of these materials in comparison with PVC products.

Some studies have reported that the DEHP released from PVC products could be decreased by modifying their surface structure under various conditions such as UV irradiation with sodium azide as an enhancer for absorbing the UV energy, gamma irradiation, an aqueous solution containing water-soluble compounds such as methacrylic acid, and gas-plasma treatment under reduced pressure.[15–17] In addition, we have reported a UV irradiation method for modifying the surface structure that can be performed easily under atmospheric conditions without reagents or special instruments.[18] These techniques suggest that the levels of DEHP migrating from a PVC product can be reduced by surface treatment without changing the type of plasticizer. This could be useful as a third choice for developing novel PVC product, but possible biological changes cannot be ignored because the surfaces of the PVC products modified by irradiation might exhibit unpredictable toxicity originating from increased oxygen content on the surface.[18] No safety evaluation of the surface-modified PVC products has been reported to date; therefore, a detailed investigation for each essential step in the development of novel PVC medical devices was performed in this study.

MATERIALS AND METHODS

Materials, chemicals, and utensils

Medical-grade PVC sheets (thickness = 0.4 mm, total contents of DEHP and MEHP = 28.7%, and 0.10 w/w) for use in blood containers were provided from Kawasumi Laboratories (Tokyo, Japan). DEHP and PVC sheets containing no additives or DEHP alone were also provided from the same company. Sandimmune® (50 mg/mL cyclosporine) and Elental-P (enteral nutrient) were purchased from Novartis Pharma K.K. (Tokyo, Japan) and Ajinomoto Pharmaceuticals Co. (Tokyo, Japan). Heparinized human blood (10,000 units/L) freshly prepared in our own laboratory according to an ethical code in National Institute of Health Sciences was also used as an extraction solvent. DEHP, DEHP-d_4, MEHP, and MEHP-d_4 were purchased from Kanto Chemical Co. (Tokyo, Japan). Phthalate-analytical-grade hexane, anhydrous sodium sulfate, and sodium chloride; dioxin-analytical-grade diethyl ether; and HPLC-grade distilled water, methanol, and acetonitrile were used in the experiments. All utensils were made of glass, metal, or Teflon® were heated at 250°C for more than 16 h prior to use.

UV irradiation

Medical-grade PVC sheet and PVC sheets containing no additives or DEHP alone were unilaterally UV-irradiated under three conditions. For condition 1, the sheet was UV-irradiated with a UV germicidal lamp placed at a distance of 60 cm (UV intensity = 52.5 $\mu W/cm^2$) for one month (integral energy density = 136 J/cm^2) on a clean bench.[18] Another PVC sheet was irradiated with a 254-nm UV lamp (Model ENF-260C/J; Spectronics Corporation, NY) at a distance of 2 cm (UV intensity = 0.45 mW/cm^2) for 25 days (integral energy density = 972 J/cm^2) for condition 2.[18] For condition 3, the PVC sample was irradiated with a 254-nm UV lamp with filter (TG-100C, 100W grid tube, 50/60 Hz, Vilber Lourmat; Marne-la-Vallée Cedex 1, France) at a distance of 2.5 cm (UV intensity = 8.3 mW/cm^2) for 4.5 h (integral energy density = 134 J/cm^2). The optimized duration (4.5 h) of UV irradiation under condition 3 was determined by the behavior of DEHP and MEHP elution from medical-grade PVC sheet UV-irradiated for various hours. In addition, DEHP in a quartz cell was UV-irradiated under condition 1. After irradiation, the samples were stored in darkness.

Elution test for DEHP and MEHP

According to the previously reported method,[18–20] medical-grade PVC sheet (1 × 3 cm, thickness = 0.4 mm) UV-irradiated unilaterally with an intensity of 8.3 mW/cm^2 was placed into a screw-capped glass tube, and 5 mL of the extraction solution (Sandimmune®, Elental-P, or heparinized blood) was added to the tube. After shaking for 1 h at room temperature, an aliquot (20 μL for DEHP and 100 μL for MEHP analyses) of the solution was removed to another glass tube; and distilled water for DEHP or 0.01 *M* HCl for MEHP (1 mL each), sodium chloride (10 mg), and 1 mL of diethyl ether containing 50 ng/mL DEHP-d_4 or MEHP-d_4 were added to the tubes. After shaking for 30 min then centrifuging at 3000 rpm for 10 min at room temperature, the organic phase was collected and dehydrated with anhydrous sodium sulfate followed by gas chromatography/mass spectrometry (GC-MS) analysis as described below. For the MEHP analysis, the sample was carboxyl-methylated with diazomethane at 0°C for 1 min prior to GC-MS analysis. MEHP analysis was also performed after washing the UV-irradiated sheets with methanol for various hours.

GC-MS analysis

The quantities of DEHP and carboxyl-methylated MEHP (MEHP-Me) in each sample were measured by GC-MS using a JEOL model JMS-700 equipped with a BPX-5 fused silica capillary column (0.22 mm × 25 m, SGE Analytical Science Pty Ltd.) at an initial temperature of 120°C for 2 min, then increasing to 300°C at 10°C/min.[21–23] The electron impact-mass spectra were recorded at 70 eV for qualitative analysis; and the ions with *m/z* 149.0240 (DEHP), 153.0492 (DEHP-d_4), 163.0395 (MEHP-Me), and 167.0647 (MEHP-d_4-Me) were selected as quantitative ions for the selected-ion mode analysis (resolution = 5000) using the lock-and-check method of calibrating standard ions (*m/z* 168.9888 of PFK). The calibration curves (n = 6) were prepared and the

quantitative data ($n = 3$) calculated using TOCO version 2.0 (total optimization of chemical operations) software and the function of mutual information theory.[21]

Fourier transform/infrared (FT-IR) and X-ray photoelectron spectroscopy (XPS) analyses

A JEOL model JIR-SPX 200 (Tokyo, Japan) was used for FT-IR spectroscopy coupled with attenuated total reflection analysis. A germanium crystal was used to analyze the PVC sheets, and the incidence angle was set at 45°. The XPS analysis was performed using a Shimadzu model ESCA-3200 (Kyoto, Japan).

LC-MS analysis and purification of the DEHP oxidants

LC-MS analysis of the DEHP UV-irradiated under condition 1 was performed with an AccuTOF™ JMS-T100LC instrument (JEOL, Tokyo, Japan) in the ESI positive-ion mode equipped with an Agilent 1100 Series HPLC system and a Capcell Pak® C8 UG 120 column (5 μm, 2 × 150 mm). Water (pump A) and methanol (pump B) containing formic acid (0.01% v/v) were used as eluents at a flow rate of 0.2 mL/min at 40°C. The gradient condition of the initial 30% B increased linearly to 95% B in 5 min then remained constant for 20 min.

The target compounds of *m/z* 371.2 and 427.2 were automatically purified using a Waters mass-triggered LC-MS collection system in the ESI positive-ion mode equipped with a YMC-Pack C8 (5 μm, 20 × 150 mm) column. Water (pump A) and methanol (pump B) containing formic acid (0.01% v/v) were used as eluents at a flow rate of 10 mL/min at room temperature. The Gradient condition of initial 30% B increased linearly to 80% B in 5 min then remained constant for 15 min.

Accurate mass and MS^n spectra of the target compound were measured using an LTQ Orbitrap XL instrument (ThermoFisher Scientific) with a direct infusion ESI positive-ion mode under the conditions of a solvent flow rate of 5 μL/min, a sheath gas flow rate of 20 arb, an auxiliary gas flow rate of 10 arb, a spray voltage of 5 kV, a capillary temperature of 275°C, a capillary voltage of 4 V, and a 60-V tube lens. A tyrosine 1,3,6 standard was used as a mass calibrant for the FT mass analyzer (resolution = 100,000), and a tyrosine 3 standard was used as a lock-mass ion (*m/z* 508.20783) during the measurements. The theoretical mass and delta value (mmu) were calculated using the elemental composition tool of Xcalibur/Qual Browser software.

NMR spectroscopy

One- and two-dimensional NMR spectra of the oxidants purified from DEHP irradiated under condition 1 were measured using a JEOL ECA600 instrument in CDCl3 at 25°C with tetramethylsilane (0.00 ppm) used as an internal standard. Proton and carbon assignments were performed by a field-gradient $^1H,^1H$-homonuclear correlation spectroscopy (COSY) experiment, $^1H,^{13}C$-heteronuclear multiple quantum coherence (HMQC) analysis, and $^1H,^{13}C$-heteronuclear multiple bond correlation (HMBC). All measurements were performed using standard JEOL software, and data processing was carried out with ALICE2 version 5.4 software.

Sterilization procedure

The surface-modified PVC sheet was sterilized by autoclaving (121°C, 15 min). Sterilization by ethylene oxide (EO) gas, H_2O_2 gas plasma, and gamma irradiation (25 kGy) under conventional conditions were entrusted to Nippo Co. (Tokyo, Japan), Johnson & Johnson K.K. (Tokyo, Japan), and Radiation Application Development Association (Gunma, Japan), respectively.

Biological tests

Medical-grade PVC sheet and PVC sheets containing no additives or DEHP alone (1 g of each) were cut into small pieces (2 × 15 mm), extracted with 10 mL minimum essential medium (MEM) supplemented with 5% FCS, nonessential amino acids, and 1 m*M* sodium pyruvate (M05) at 37°C for 24 h for the cytotoxicity test, and with 5 mL Eagle's MEM supplemented with 10% heat-inactivated FCS at 37°C for 48 h for the *in vitro* chromosome aberration (CA) test, then separated from the extract by decantation followed by serial dilution with the medium.

The cytotoxicity test was carried out according to a previously reported method.[22] Chinese hamster fibroblast V79 cells were seeded at 50 cells/well in 24-well plates, and incubated at 37°C in the humidified atmosphere. After 24 h of incubation, the medium was exchanged with 1 mL of the serially diluted medium extract or the medium without the extract (for a control), and the cells were cultured for another 6 days. The formed colonies were fixed with a 10% formalin solution and stained with 5% Giemsa staining solution. The colonies in each well were counted, and the relative plating efficiency was calculated as the ratio of the number of colonies in the sample to that in the control. The IC_{50} value was calculated by the probit method.

The *in vitro* CA test was carried out according to a previously reported method.[23] The Chinese hamster lung cells were seeded at 1.0×10^5/plate (60-mm diameter) and incubated for 24 or 48 h with several concentrations of the extract or medium. Colcemid (0.2 μg/mL) was added for the final 2 h. Chromosomes were prepared as previously reported.[24] All slides were coded, and the number of cells with structural CAs in the 100 well-spread metaphases was counted. The experiments were repeated at least twice and the representative data are shown.

RESULTS

Analysis of surface structure

FT-IR spectra of the PVC sheets treated with or without UV irradiation were recorded. Figure 1 shows a characteristic absorption band at 635 cm^{-1} that is due to the C—Cl stretching vibration from PVC in the FT-IR spectrum of non-irradiated medical-grade PVC sheet (control). Other characteristic absorptions originating from the C—H bond of the aromatic compound, the carbonyl group from DEHP, and the alkane C—H bond of PVC and DEHP were observed at 742, 1720, and 1250 cm^{-1}, respectively. In contrast, the PVC

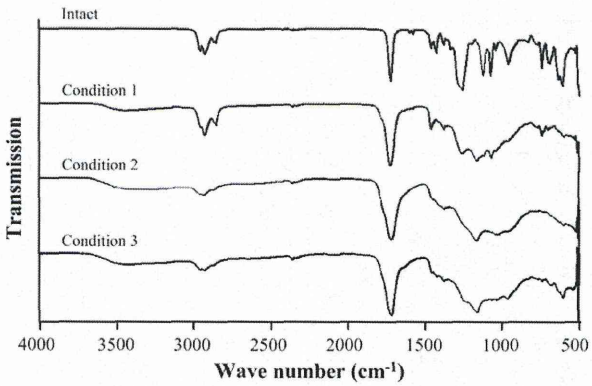

FIGURE 1. FT-IR spectra of control and UV-irradiated PVC sheets. Characteristic absorptions of PVC containing DEHP were observed at 635 (C—Cl bond), 742 (aromatic C—H bond), 1720 (carbonyl group of DEHP), and 1250 (alkane C—H bond) cm^{-1} in the spectrum of the control PVC sheet. PVC sheets irradiated under conditions 1, 2, and 3 were found to exhibit broadened absorption bands.

sheet irradiated under condition 1 was found to exhibit broadened absorption bands (Fig. 1), and the FT-IR spectra of the PVC sheets irradiated under conditions 2 and 3 exhibited additional broadening (Fig. 1). The FT-IR spectrum of the non-irradiated side was identical to the control PVC sheet, indicating that there was no change in its surface structure (data not shown).

The elemental composition of each PVC sheet was determined by XPS analysis. As shown in Figure 2, carbon, oxygen, chlorine, and silicon atoms were found on the control PVC sheet surface. In contrast, increased oxygen content and a disappearance of chlorine were observed on the surface of the PVC sheet irradiated under condition 1. In addition, the degree of surface oxidation was enhanced by UV irradiation under condition 2, and the carbon content was decreased relative to the increase in oxygen content. The composition ratios of the PVC sheets irradiated under conditions 2 and 3 were nearly identical.

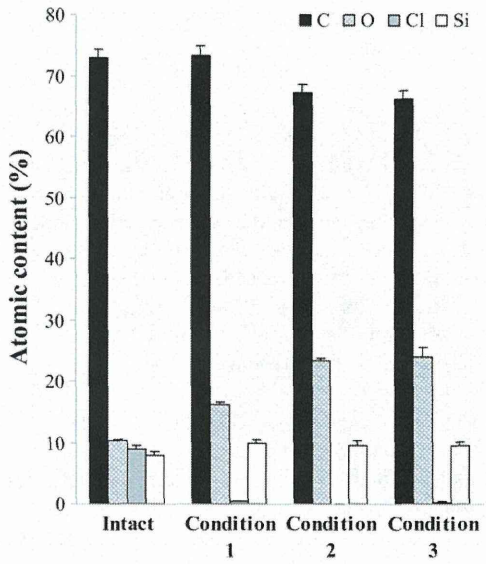

FIGURE 2. Results of the XPS analysis of control and UV-irradiated PVC sheets under conditions 1, 2, and 3. Carbon, oxygen, chlorine, and silicon atoms were found on the control PVC sheet surface. In contrast, an increase in oxygen content and the disappearance of chlorine were observed on the surface of the PVC sheet irradiated under conditions 1, 2, and 3.

Cytotoxicity and *in vitro* CA tests

To evaluate biological safety, the cytotoxicity of each PVC sheet was estimated. As shown in Figure 3, no cytotoxicity was observed in a control PVC sheet (IC_{50} > 100%), but a PVC sheet irradiated under condition 1 exhibited significant toxicity in a dose-dependent manner (IC_{50} = 22.2%), and the toxicity was enhanced by the irradiation under condition 2 (IC_{50} = 7.8%). In contrast, the PVC sheet irradiated under condition 3 exhibited weak toxicity (IC_{50} = 83.1%) compared with the sheets irradiated under conditions 1 and 2.

A CA test was also performed to evaluate the biological properties of each PVC sheet. Although no induction of CAs was observed in a control PVC sheet PVC sheet, Tables I and II show that irradiation under condition 1 induced a significant frequency of CAs in the PVC sheet. The latter sheet showed a positive response over a short treatment of 6 h because the frequency of polyploidy significantly increased in a concentration-dependent manner, and the total CA frequency reached 5.0% (Table II). In the continuous treatment of the PVC sheet under condition 1, polyploidy was not induced during 24 h of treatment, but the frequency of chromatid breaks and exchanges significantly increased, and the total CA frequency was over 10.0%. In addition to chromatid exchanges, polyploidy was also detected after 48 h of treatment. In contrast, the PVC sheet irradiated under condition 3 did not induce a significant frequency of CAs as shown in Table III.

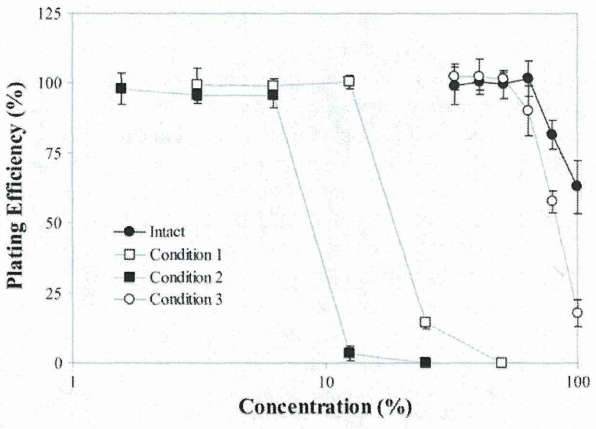

FIGURE 3. Results of cytotoxicity tests of control and UV-irradiated PVC sheets under conditions 1, 2, and 3. Although no cytotoxicity was observed in the control PVC sheet (●), significant cytotoxicity was found in the PVC sheet irradiated under conditions 1 (IC_{50} = 22.2%) (□) and 2 (IC_{50} = 7.8%) (■). However, the PVC sheet irradiated under condition 3 exhibited weak toxicity (IC_{50} = 83.1%) (○).

TABLE I. Results of the *In Vitro* CA Test of a Control PVC Sheet

Treatment Time (h)	Concentration (%)	Frequency of Polyploidy (%)	Frequency of Cells with Chromosome Aberrations (%)						
			ctg	ctb	cte	f	csb	cse	total
6	0	0	1	0	1	0	0	0	2
	25	2	0	0	0	0	0	0	0
	50	1	0	1	0	0	0	0	1
	75	2	0	0	0	0	0	0	0
	100	0	0	0	1	0	0	0	1
24	0	1	0	0	0	0	0	0	0
	25	2	1	0	1	0	1	0	3
	50	2	0	0	0	0	0	0	0
	75	2	1	0	0	0	0	0	1
	100	2	0	1	0	0	0	0	1

[a]ctg, chromatid gaps. ctb, chromatid breaks. cte, chromatid exchanges. f, fragmentation. csb, chromosome breaks. cse, chromosome exchanges.

No significant frequency of CAs was observed.

Identification of toxic compounds

Figure 4(c) shows that the PVC sheet containing no additives did not exhibit any cytotoxicity even after UV irradiation under condition 1. In contrast, the toxicity of the control PVC sheet and the PVC sheet containing DEHP alone was increased from IC_{50} = 60.3% to IC_{50} = 23.4% and IC_{50} = 79.4% to IC_{50} = 29.5%, respectively, by the UV irradiation [Fig. 4(a,b)]. These results indicated that some toxic compounds resulted from the UV irradiation of the DEHP molecule under condition 1.

In ESI-LC/MS analysis of the DEHP standard in the infusion mode, characteristic ions were observed at *m/z* 279.1 $[M+H\text{-ethylhexyl}]^+$, 391.3 $[M+H]^+$, 413.2 $[M+Na]^+$, 429.2 $[M+K]^+$, and 803.5 $[2M+Na]^+$ as shown in Figure 5(a). In addition to these ions, unknown peaks were detected at *m/z* 371.2 $[M+Na]^+$ (compound A) and 427.2 $[M+Na]^+$ (compound B) in the ESI-MS spectrum of the DEHP irradiated under condition 1 [Fig. 5(b)]. As shown in Figure 6, MS^n analysis of the ions revealed that compounds A and B were analogues of DEHP because the product ions detected at *m/z* 259.1 and *m/z* 315.1 in the MS^2 analyses of the parent ions were assigned to the sodium-adducted molecular species eliminated the ethylhexyl group. The peak at *m/z* 301.1 detected in the MS^2 spectrum of *m/z* 472.2 was assigned as the sodium-adducted ion of the MEHP molecule, indicating that one of ethylhexyl chains in the DEHP molecule was not structurally altered by the UV irradiation. The product ions corresponding to the hydrogen- or sodium-adducted molecular species of phthalic acid were detected at *m/z* 167.0 and 188.9 in the MS^3 spectra of *m/z* 427.2/301.1 and *m/z* 427.1/315.1. In addition, the product ion at *m/z* 170.9 detected in the MS^3 analyses of *m/z* 371.2/259.1

TABLE II. Results of the *In Vitro* CA Test of a PVC Sheet UV-Irradiated Under Condition 1

Treatment Time (h)	Concentration (%)	Frequency of Polyploidy (%)	Frequency of Cells with Chromosome Aberrations (%)						
			ctg	ctb	cte	f	csb	cse	total
6	0	1	0	0	0	0	0	0	0
	10	0	0	0	0	0	0	0	0
	20	2	0	0	0	0	0	0	0
	40	7	0	1	0	0	0	0	1
	50	25	0	1	4	0	1	0	5
24	0	3	0	0	0	0	0	0	0
	20	1	0	0	0	0	0	0	0
	40	4	4	24	6	0	0	0	29
	60								Tox
	80								Tox
48	0	1	0	1	0	0	0	0	1
	20	1	1	0	0	0	0	0	1
	40	10	1	3	6	0	0	0	9
	60								Tox
	80								Tox

[a]ctg, chromatid gaps. ctb, chromatid breaks. cte, chromatid exchanges. f, fragmentation. csb, chromosome breaks. cse, chromosome exchanges. Tox, cell death.

The sheet induced a significant frequency of CAs in both the short time and continuous treatment.

TABLE III. Results of the *In Vitro* CA Test of a PVC Sheet UV-Irradiated under Condition 3

Treatment Time (h)	Concentration (%)	Frequency of Polyploidy (%)	Frequency of Cells with Chromosome Aberrations (%)						
			ctg	ctb	cte	f	csb	cse	total
6	0	1	0	0	0	0	0	0	0
	20	2	1	1	0	0	0	0	2
	40	1	0	0	0	0	0	0	0
	60	0	2	0	0	0	0	0	2
	80	1	2	0	0	0	1	1	4
	100	2	1	2	0	0	0	0	3
24	0	1	0	1	0	0	0	0	1
	20	1	2	1	0	0	0	1	4
	40	1	2	0	0	0	0	0	2
	60	0	3	0	0	0	0	0	3
	80	1	2	1	0	0	0	0	3
	100								NA
48	0	1	1	0	0	0	0	0	1
	20	1	0	0	0	0	0	0	0
	40	0	0	1	0	0	0	0	1
	60	1	0	0	0	0	0	0	0
	80								NA
	100								Tox

[a]ctg, chromatid gaps. ctb, chromatid breaks. cte, chromatid exchanges. f, fragmentation. csb, chromosome breaks. cse, chromosome exchanges. NA, not analyzable due to shortage of metaphase cells. Tox, cell death.

The sheet did not induce a significant frequency of CAs.

and *m/z* 427.1/301.1 was identified as a fragment derived from the sodium-adducted phthalic anhydride.

Compounds A and B were purified using a mass-triggered LC-MS collection system in which they were eluted at 11.9 min as a single peak and approximately 12.7 min as a peak with a shoulder. The final yields were 0.4 and 4.8% for compounds A and B, respectively. The DEHP was simultaneously separated by the collection system as a reference (retention time = 14.8 min, yield = 70.1%). As shown in Figure 7, the IC_{50} values from the cytotoxicity tests of the purified DEHP and compounds A and B were 242 μg/mL, 46.0 μg/mL, and 18.8 μg/mL, respectively, indicating that the cytotoxicities of compounds A and B were approximately 5-times and 13-times stronger than that of DEHP.

The ^{1}H- and ^{13}C-NMR spectra of the purified compounds A and B were recorded to identify their chemical structures, and each signal was fully assigned by COSY, HMQC, and HMBC analyses. The NMR spectra of DEHP were also measured as a reference. As shown in Figure 8(c,d), NMR spectroscopy clearly identified compound A as 2-ethylhexyl-2-keto-butyl phthalate because the spectra were similar to those of DEHP [Fig. 8a,b)]. The characteristic signals were detected at 4.88 ppm (*s*, —O—CH_2—CO—), 2.53 ppm (*q*, J 7.56 Hz, —CO—CH_2CH_3), and 1.13 ppm (*t*, J 7.57 Hz, —CO—CH_2CH_3) in ^{1}H-NMR analysis [Fig. 8(c)]; and three types of carbonyl carbon atoms were observed at 204.4 ppm (—O—CH_2—CO—), 167.3 ppm (Ph-COO-Ethylhexyl), and 167.1 ppm (Ph-COO-oxidized chain) in the ^{13}C-NMR spectrum [Fig. 8(d)]. A terminal methyl carbon (—CO—CH_2CH_3) of the oxidized chain was recorded at 7.11 ppm, in addition to the peaks at 10.97 ppm and 14.07 ppm corresponding to the ethyl- and hexyl-group terminals of the ethylhexyl chain [Fig. 8(d)]. This assignment was also supported by accurately measuring the mass ($C_{20}H_{28}O_5Na$: theoretical mass = *m/z* 371.18290 $[M+Na]^+$, measurement mass = *m/z* 371.18297 $[M+Na]^+$, Delta = 0.07 mmu). In contrast, the NMR spectroscopy indicated that the purified compound B fraction contained several species of DEHP oxidants. Four types of carbonyl carbons formed by the individual oxidation of position 5, 7, 4, or 3 in the ethylhexyl chain were observed in the ^{13}C-NMR analysis at 208.7, 209.7, 210.5, and 211.6 ppm, respectively [Fig. 8(f)]. In addition, several types of carbonyl carbons (Ph-COO—) originating from the phthalic acid backbone were detected in the range of 167.3–167.9 ppm on behalf of single peak at 167.8 ppm derived from the carbon atom in the DEHP molecule [Fig. 8(f,b)]. As shown in Figure 8(e), although the ^{1}H-NMR spectrum of compound B was similar to that of the DEHP standard, two proton signals were detected at 2.13 (s, —CH_2—CO—CH_3) and 2.22 ppm (s, >CH—CO—CH_3). These signals derived from the terminal methyl groups contiguous to the carbonyl groups formed by individual oxidation of position 5 or 7 in the ethylhexyl chain. The methyl protons of the nearby carbonyl group were also detected in the range from 1.01 to 1.09 ppm (*t*, J 7.57 Hz). Furthermore, methine protons contiguous to the carbonyl groups of position 3 or 7 were recorded in the range of 4.42–4.47 ppm (*m*), and methylene protons contiguous to the carbonyl groups of position 3, 4, or 5 were detected at 2.39–2.56 ppm (*m*) [Fig. 8(e)]. These signals were shifted to a lower field compared with the chemical shifts of the original methyl, methylene, and methine protons in the DEHP

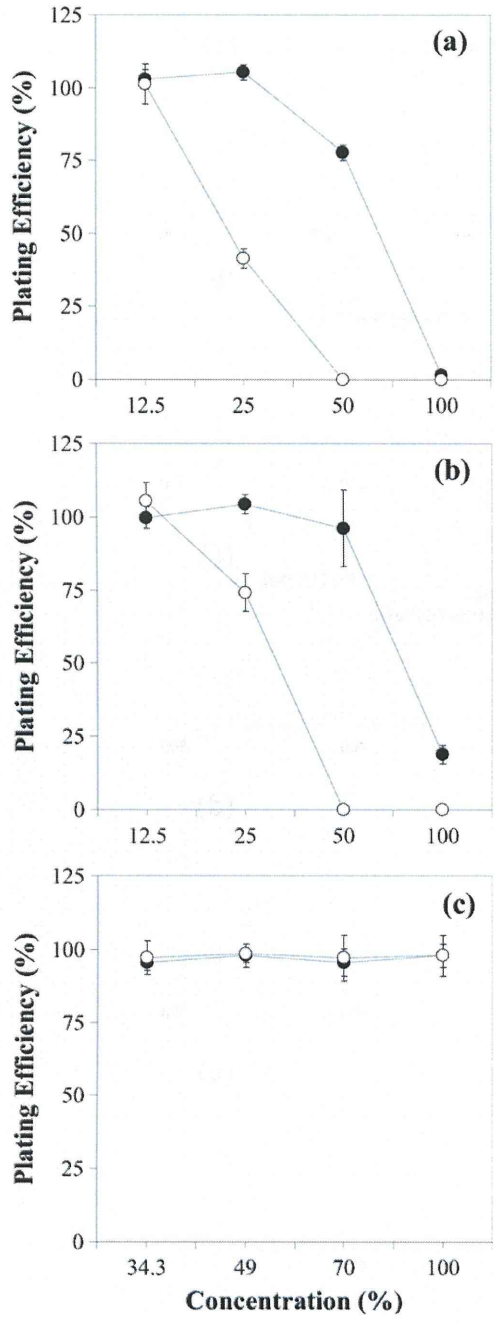

FIGURE 4. The change in cytotoxicity of a medical-grade PVC sheet for use as a blood container, a PVC sheet containing DEHP alone, and a PVC sheet containing no additives, before (●) and after (○) UV irradiation under condition 1. The PVC sheet containing no additives exhibited no cytotoxicity even after the UV irradiation (c). In contrast, the toxicity of the control PVC sheet (a) and the PVC sheet containing DEHP alone (b) increased from IC_{50} = 60.3% to IC_{50} = 23.4% and IC_{50} = 79.4% to IC_{50} = 29.5%, respectively, with UV irradiation.

molecule [Fig. 8(a,e)]. These data and the result of the HMBC analysis (Fig. 9) revealed that compound B was a mixture of four types of partially oxidized DEHP molecules in which the original methylene group at position 3, 4, 5, or 7 in the ethylhexyl chain was individually converted into a carbonyl group. The accurate mass analysis supported this assignment and revealed that these oxidants had the same chemical composition ($C_{24}H_{36}O_5Na$: theoretical mass = *m/z* 427.24550 $[M+Na]^+$, measurement mass = *m/z* 427.24540 $[M+Na]^+$, Delta = 0.10 mmu) because the purified compound B was detected as a single peak in the LC-MS analysis in the infusion mode.

DEHP and MEHP migration test

The elution behavior of the DEHP from a PVC sheet UV-irradiated unilaterally with an intensity of 8.3 mW/cm^2 was estimated. DEHP and MEHP were quantified by GC-MS analysis using DEHP-d_4 and MEHP-d_4 as an internal standard. Sandimmune®, human blood, and Elental-P were used as the extraction solvents and contained DEHP and MEHP in concentrations of 0.70 and 0.27 μg/mL, 0.24 and 0.33 μg/mL, and 0.54 and 0.32 μg/mL, respectively, as a background.

As shown in Figure 10(a), the amounts of DEHP released from the PVC sheet by Sandimmune® extraction decreased with increasing duration of UV irradiation, and the initial concentration was nearly halved after 4 h. The

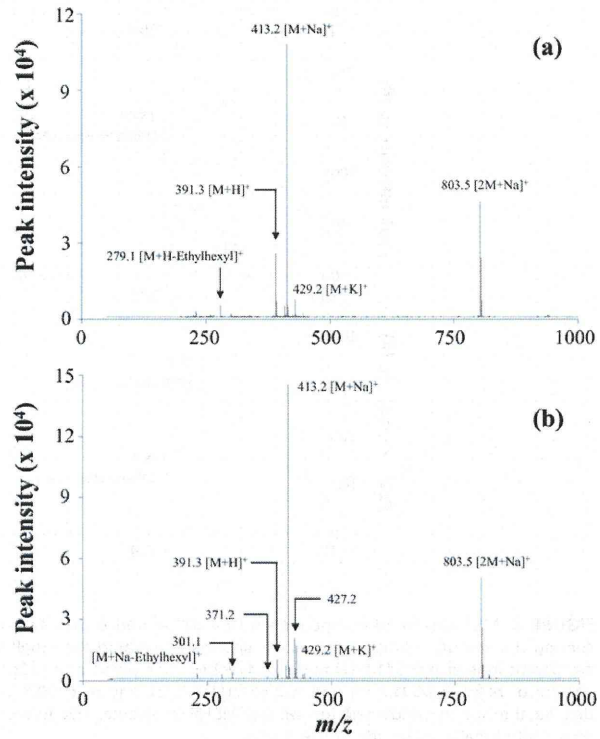

FIGURE 5. ESI-MS spectra of DEHP measured in the direct infusion mode, before and after UV irradiation under condition 1. The characteristic ions were observed at *m/z* 279.1 $[M+H\text{-ethylhexyl}]^+$, 391.3 $[M+H]^+$, 413.2 $[M+Na]^+$, 429.2 $[M+K]^+$, and 803.5 $[2M+Na]^+$ in the spectrum of the DEHP standard (a). In addition to these ions, unknown peaks were detected at *m/z* 371.2 $[M+Na]^+$ and 427.2 $[M+Na]^+$ in the spectrum of the DEHP irradiated under condition 1 (b).

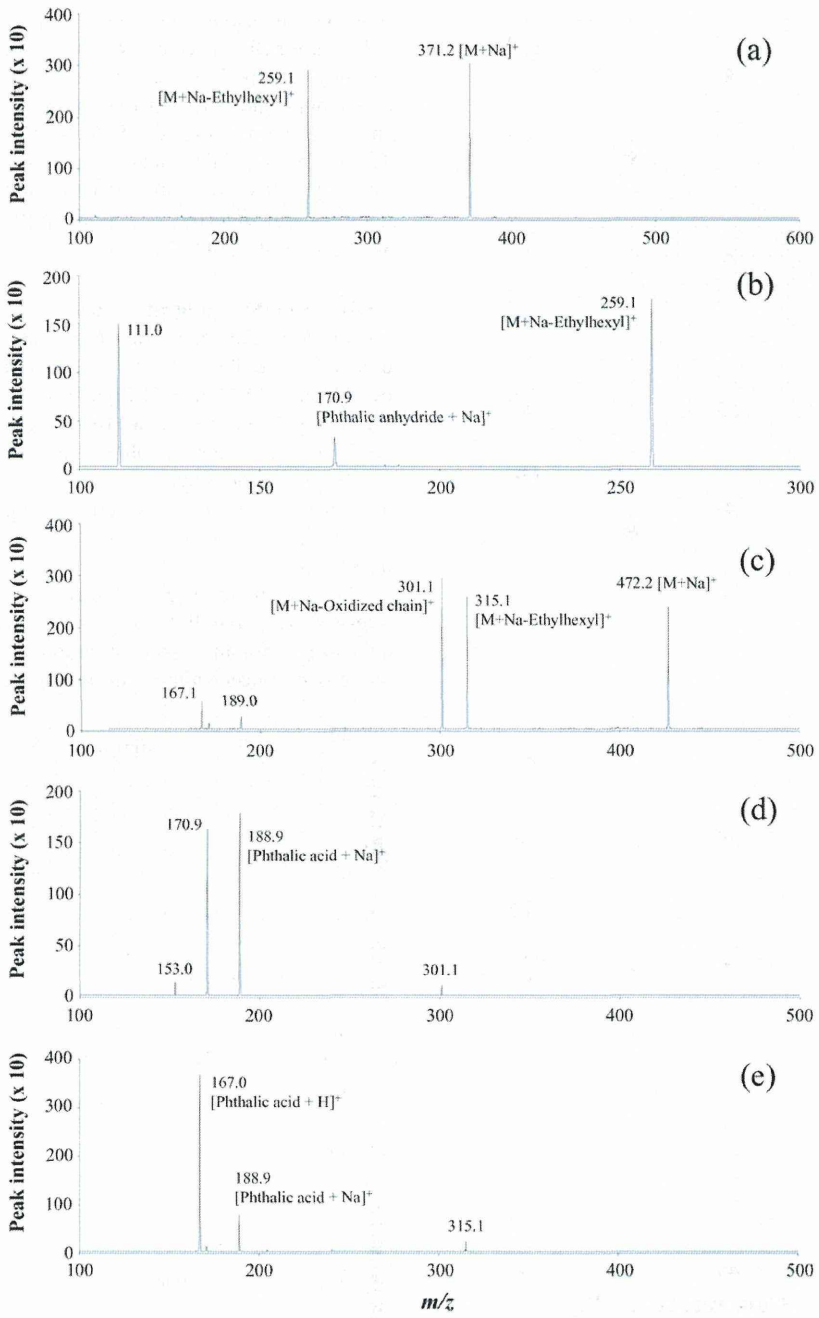

FIGURE 6. MS^n spectra of compounds A (*m/z* 371.2) and B (*m/z* 472.2) purified via a mass-triggered collection system. The product ions representing the sodium-adducted molecular species eliminated the ethylhexyl group were detected at *m/z* 259.1 and *m/z* 315.1 in MS^2 analyses of the parent ions at *m/z* 371.2 (a) and *m/z* 472.2 (c). The peaks at *m/z* 301.1 detected in MS^2 spectrum of *m/z* 472.2 (c), *m/z* 167.0 and 188.9 in MS^3 spectra of *m/z* 427.2/301.1 (d) and *m/z* 427.1/315.1 (e), and *m/z* 170.9 in MS^3 analyses of *m/z* 371.2/259.1 (b) and *m/z* 427.1/301.1 (d) were identified as the sodium-adducted ion of the MEHP molecule, the hydrogen- or sodium-adducted molecules of phthalic acid, and the sodium-adducted phthalic anhydride, respectively.

quantities of DEHP eluted from the sheet irradiated for 4.5 h under condition 3 extracted in human blood and Elental-P were also reduced from 3.08 to 1.55 μg/mL and 22.6 to 9.24 μg/mL, respectively [Fig. 10(b)]. These results indicated that DEHP elution was significantly suppressed on the UV-irradiated side of the PVC sheets.

Although little release of MEHP from the PVC sheet was observed prior to the UV irradiation, the release increased

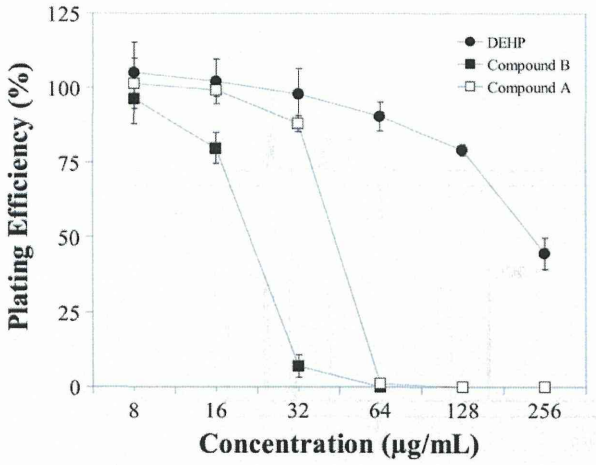

FIGURE 7. Results of the cytotoxicity test of DHEP (●), compounds A (□) and B (■) purified by mass-triggered collection system. The degree of cytotoxicity of compounds A (IC_{50} = 46.0 μg/mL) and B (IC_{50} = 18.8 μg/mL) were approximately 5- and 13-times stronger than that of DEHP (IC_{50} = 242 μg/mL).

significantly after the UV irradiation as shown in Figure 11(a,b). Figure 11(c), however, shows that the MEHP generated from the DEHP by UV irradiation was easily removed by washing the sheet with methanol, and the amount released decreased almost to the background level after washing for 0.5 h.

Selection of a sterilization method

To select the applicable methods for sterilizing the surface-modified PVC products, the plasticizer elution and cytotoxicity before and after sterilization were estimated. The PVC sheet irradiated unilaterally under condition 3, then washed with methanol for 10 min was sterilized by autoclave, EO gas, H_2O_2 gas plasma, and gamma irradiation under the conventional conditions. As shown in Figure 12, the amount of DEHP eluted from the sheets with Sandimmune® extraction were almost half that of the control PVC sheets regardless of the sterilization method. After gamma-ray sterilization, the amount of MEHP eluted from the UV-irradiated sheet was half that of control PVC sheet [Fig. 12(d)]. In contrast, although little elution of MEHP from the control PVC sheet was detected following sterilization by autoclave, EO gas, and H_2O_2 gas plasma, the MEHP elution was significantly increased in the surface-modified PVC sheet sterilized via these three methods [Fig. 12(a,b,c)].

The IC_{50} values in the cytotoxicity test of the control PVC sheet sterilized via autoclave, EO gas, H_2O_2 gas plasma, and gamma irradiation were 77.3, >100, 95.6, and 85.9%, respectively. In contrast, the cytotoxicity of the surface-modified PVC sheet was slightly enhanced with sterilization, and the values were 71.8, 86.7, 82.5, and 77.9%, respectively, although all were below the level allowable for use in medical devices.

DISCUSSION

This investigation attempted to study the suppression of plasticizer migration in PVC medical devices via surface modification with UV irradiation. DEHP elution from PVC products is known to decrease or be eliminated by modifying the surface structure with physicochemical treatments such as UV and gamma irradiation.[15–17] The photochemical degradation with UV/H_2O_2 could be an efficient method to remove DEHP in water.[25] As shown in these reports and the present study, the mechanism by which the DEHP elution is suppressed could involve cross linking that accompanies oxidation and the elimination of chlorine on a thin layer of the PVC surface. The techniques reported to date are useful for surface modification, but are not linked to the development of novel products possibly because some toxicities are thought to arise from oxidation that accompanies the treatment. The present study clearly shows that excrescential toxicity occurred in the PVC sheet irradiated under condition 1 identical to a previously reported technique.[18] However, we found that the occurrence of unexpected toxicity could be suppressed to a negligible level with condition 3. The integral energy density was the same in conditions 1 and 3, but the intensity of the UV lamp and irradiation time were different, indicating that UV irradiation using a strong UV source for a short duration was useful in preventing toxicity. The reason that the toxicity did not increase with condition 3 is not well understood because the oxygen content on the surface of the PVC sheet treated under condition 3 was higher than that of the sheet irradiated under condition 1. The PVC sheet treated under condition 2 exhibited a higher toxicity than that of the PVC sheet treated under condition 1, despite having an oxidation level nearly identical to that of the PVC sheet irradiated under condition 3. Given these results, one can speculate that adequately strong UV irradiation over a short duration, in comparison with long-term weak irradiation, might enhance the formation of a cross-linked structure, and toxic compounds might be taken into the structure and fixed.

The results of the cytotoxicity test using PVC sheets containing no additives and DEHP alone clearly indicated that the toxic compounds were formed from the DEHP molecule by the UV irradiation. Mass spectrometry and NMR spectroscopy demonstrated that DEHP oxidants with significant cytotoxicity such as compounds A and B were generated by UV irradiation. Although other compounds not identified in this study might be responsible for the toxicity of the PVC sheet irradiated under conditions 1 and 2, compounds A and B were clearly involved in the toxicity because the cytotoxicities of these compounds were approximately 5- and 13-times stronger than that of DEHP. Although MEHP, responsible for the toxicity of DEHP in rodents, was also generated by the UV irradiation, the MEHP was effectively and easily removed by washing the sheet with methanol for a short time (10 min was sufficient) after irradiation.

PVC medical devices are sterilized during the final step of their manufacture, and autoclave or gamma irradiation techniques have been used as convenient methods for the sterilization. We researched the applicable methods for

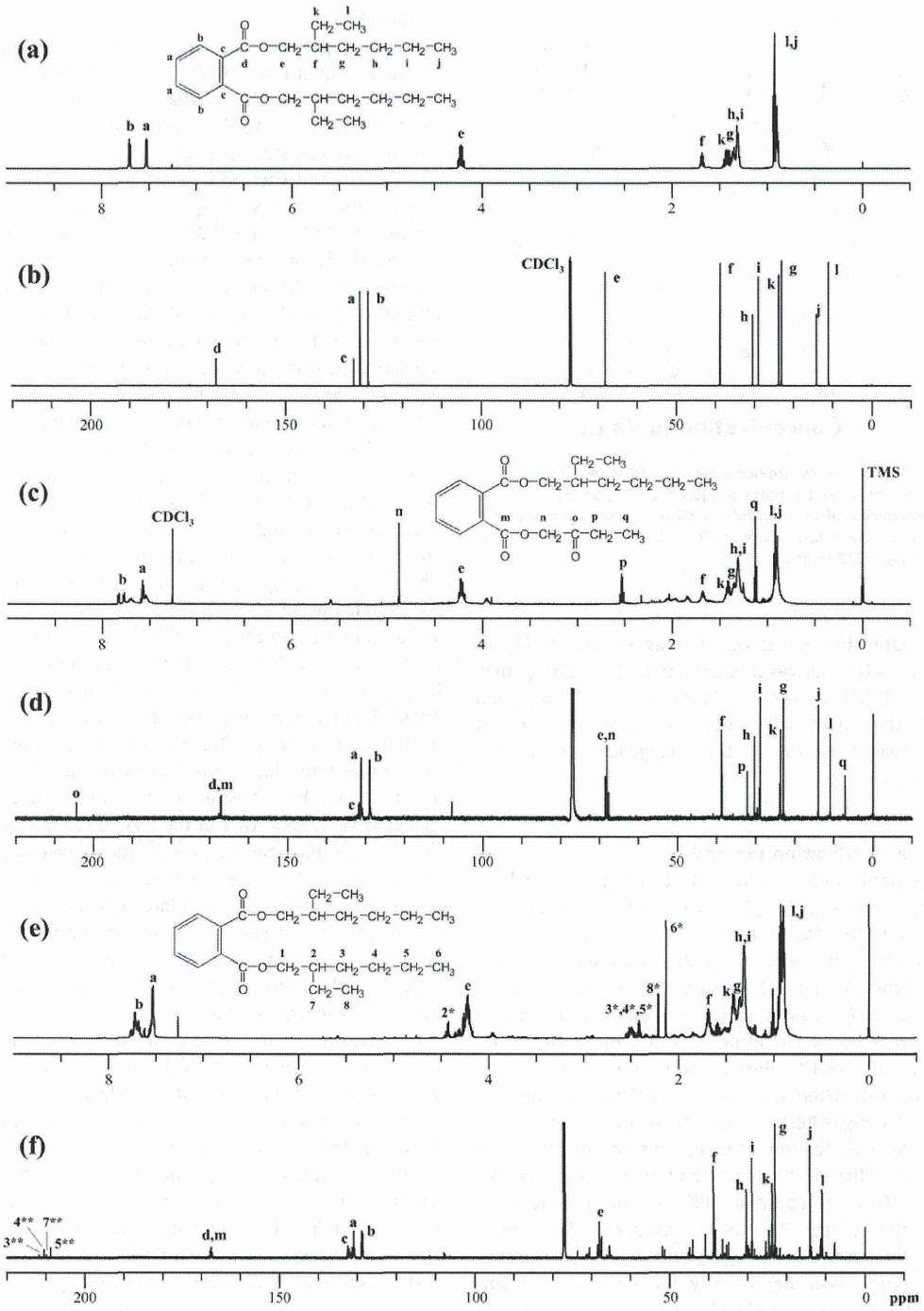

FIGURE 8. ^{1}H- and ^{13}C-NMR spectra of DEHP, compounds A and B purified via the mass-triggered collection system. Each signal was fully assigned by COSY, HMQC, and HMBC analyses. Compound A was clearly identified as 2-ethylhexyl-2-keto-butyl phthalate because the characteristic signals were detected at 4.88 ppm, 2.53 ppm and 1.13 ppm in the ^{1}H-NMR spectrum (c) and at 204.4 ppm and 7.11 ppm in the ^{13}C-NMR spectrum (d) in addition to each signal derived from the DEHP molecule (a and b). Four types of carbonyl carbons (5**, 7**, 4**, 3**) formed by the individual oxidation of the ethylhexyl chain were observed at 208.7, 209.7, 210.5, and 211.6 ppm in the ^{13}C-NMR spectrum (f) of the compound B fraction, and several types of carbonyl carbons originating from the phthalic acid backbone were also detected in the range from 167.3 to 167.9 ppm (f). In the ^{1}H-NMR spectrum (e) of the compound B fraction, two proton signals (6* and 8*) corresponding to the terminal methyl groups contiguous to the carbonyl group present at position 5 or 7 were detected at 2.13 and 2.22 ppm, and several proton signals representing methylene (3*, 4*, 5*: 2.39 to 2.56 ppm) and methine (2*: 4.42 to 4.47 ppm) groups contiguous to the carbonyl groups also appeared in a lower field in the ^{1}H-NMR spectrum (e). These results indicated that compound B was a mixture of four types of partially oxidized DEHP molecules in which the original methylene group of positions 3, 4, 5, or 7 in the ethylhexyl chain was individually converted into a carbonyl group.

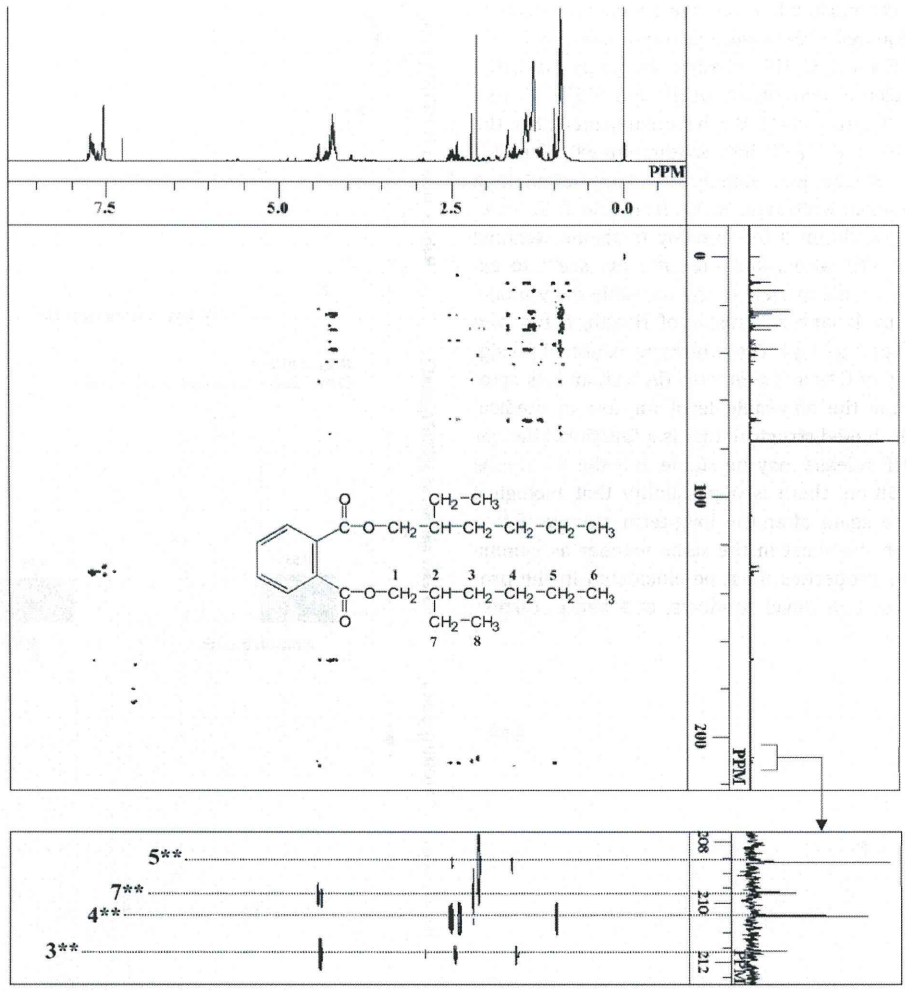

FIGURE 9. HMBC spectrum of the compound B fraction purified via a mass-triggered collection system. The methylene group of position 3, 4, 5, or 7 in the ethylhexyl chain of the DEHP molecule was individually exchanged to a carbonyl group (3**, 4**, 5**, or 7**) by UV irradiation under condition 1 because the characteristic 2- and 3-bond CH long-range couplings were detected in the HMBC spectrum.

sterilizing surface-modified PVC sheets because factors such as heat, chemicals, and radioactivity during the sterilization might affect the modified surface structure. The physicochemical properties of the UV-irradiated surface were found to remain unchanged with regard to the suppression of DEHP elution following the sterilization methods used in this study. The DEHP present in PVC products has been reported to partially convert into MEHP by sterilization with gamma irradiation,[26] and hence, the quantity of MEHP eluted from a control PVC sheet after gamma-ray sterilization was slightly increased in comparison with that of sheets sterilized by autoclave, EO gas, and H_2O_2 gas plasma. Following gamma-ray sterilization, however, the amount of MEHP eluted from a PVC sheet treated under condition 3 was half that of the control PVC sheet, indicating that the surface structure of the UV-irradiated side was not destroyed and the release of MEHP from the side was effectively suppressed even after gamma-ray sterilization. Although the permeability of UV waves and gamma rays are different, their mechanisms for killing micro-organisms and forming cross-linkages between PVC molecules are similar, and hence, the physicochemical properties of the UV-irradiated PVC sheet may not be influenced by gamma irradiation. In contrast, some structural changes in the UV-irradiated surface might be induced by heat treatment (autoclave) and chemicals (EO gas and H_2O_2 gas plasma) because the release of MEHP from the surface-modified PVC sheet was found to increase after these sterilizations.

The technique presented in this study may be useful for improving the biological safety of PVC medical devices and will eliminate the need for biologically safe alternate plasticizers. The PVC sheets were slightly yellowed by the UV irradiation, but their transparency was maintained throughout treatment. The dynamic properties of the UV-irradiated PVC sheets were nearly identical to those of a control PVC sheet as determined by tensile tests and their static contact angle

to water.[18] The thermostability and the chemical resistance of the surface-modified sheets were also improved over that of the control PVC sheet. DEHP exposure should be estimated as the sum of release amounts of DEHP and MEHP in risk assessment of PVC products.[26] We have confirmed that the migration of DEHP and MEHP into Sandimmune®, Elental-P, and fetal bovine serum was significantly suppressed in a novel blood-container prototype made from the PVC sheet irradiated under condition 3 followed by methanol washing and gamma-ray sterilization, and the amounts seem to exhibit no risk for patients in view of the tolerable daily intake value restricted by Japanese Ministry of Health, Labor and Welfare (40–140 μg/kg/day). The prototype exhibited no significant frequency of CAs in the *in vitro* CA test, and its cytotoxicity was below the allowable level for use in medical devices. The cross-linked structure that is a functional barrier to suppress DEHP release may be stable, but the lifetime is unknown. In addition, there is a possibility that biological toxicity may arise again after the long-term storage if free radical remains in the sheet in the same manner as gamma irradiation. These properties must be elucidated in the process of development of novel products, and hence, further estimation including the long-term stability of novel blood container consisted of PVC sheet UV-irradiated under condition 3 is now in progress in our laboratory. These data will be reported elsewhere.

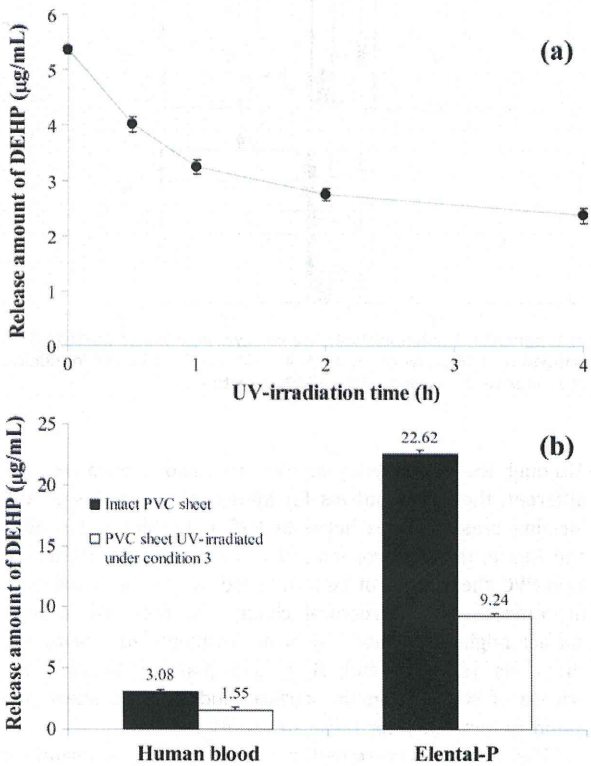

FIGURE 10. Elution behavior of DEHP from a PVC sheet unilaterally irradiated with a UV intensity of 8.3 mW/cm^2. The quantity of DEHP released from the PVC sheet by Sandimmune® extraction (a) reached nearly half its initial concentration after UV irradiation for 4 h. The quantities of DEHP eluted from the sheet irradiated under condition 3 extracted in human blood and Elental-P (b) were reduced in the same manner. These results indicated that the DEHP release from the UV-irradiated side was significantly suppressed.

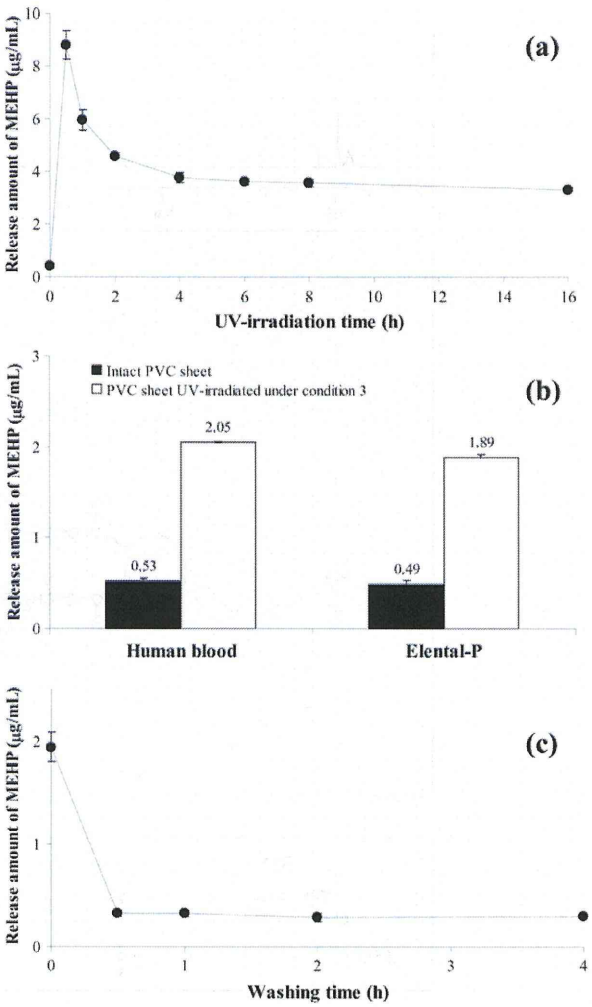

FIGURE 11. Elution behavior of the MEHP from a PVC sheet unilaterally irradiated with a UV intensity of 8.3 mW/cm^2. A portion of the DEHP was converted into MEHP by the UV irradiation, and a significant release of MEHP was observed in the elution test with Sandimmune® extraction (a). A release from the PVC sheet irradiated under condition 3 was also recognized in the extraction test using human blood and Elental-P (b). However, the MEHP generated by the irradiation was easily removed via methanol washing (c).

CONCLUSIONS

UV irradiation using a strong UV-source over a short duration followed by a methanol rinse and gamma-ray sterilization might be useful for preparing novel PVC medical devices that did not elute plasticizers and do not incur excrescential toxicity. This is a first report for the total development of novel PVC medical devices that have been surface-modified with UV irradiation.

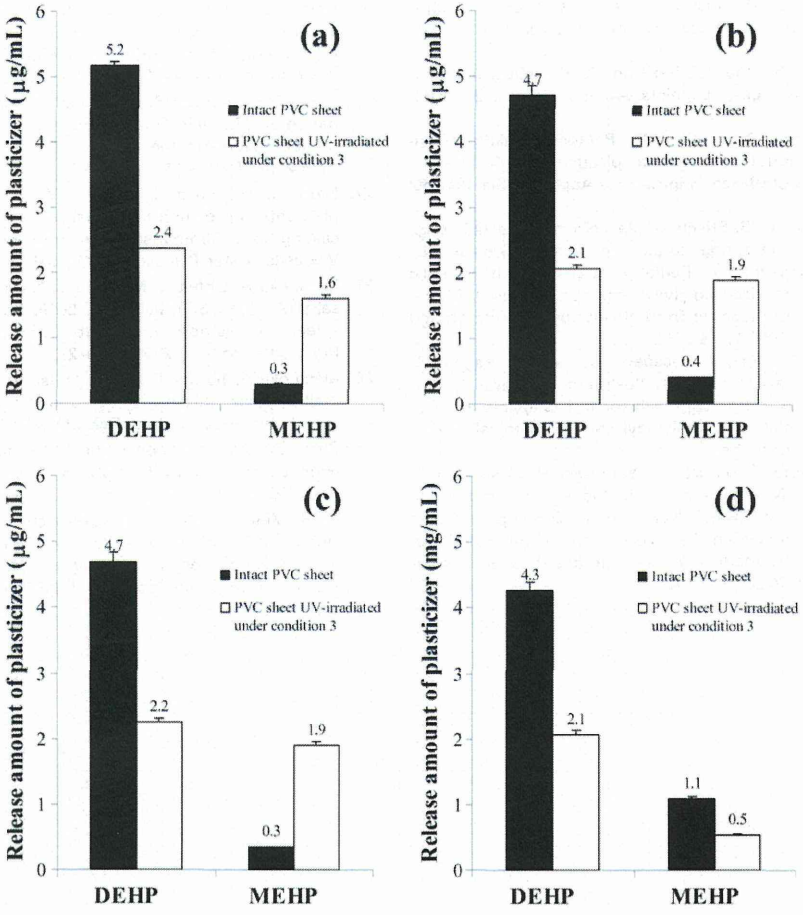

FIGURE 12. Effect of sterilization on the elution behavior of DEHP and MEHP from a PVC sheet irradiated under condition 3 followed by methanol washing. The quantities of DEHP eluted from the sheets with Sandimmune® extraction were nearly half that of the control PVC sheets sterilized by each method (a–d), indicating that the physicochemical properties of the UV-irradiated surface with regards to the suppression of DEHP elution were maintained even after the sterilizations. In addition, the surface structure for the suppression of MEHP release was not affected by gamma-ray sterilization (d). In contrast, although little elution of MEHP from the control PVC sheet was detected after autoclave, EO gas, and H_2O_2 gas-plasma sterilizations, the MEHP elution was significantly increased in the surface-modified PVC sheet sterilized by autoclave (a), EO gas (b), and H_2O_2 gas plasma (c).

REFERENCES

1. Allwod MC. The release of phthalate ester plasticizer from intravenous administration sets into fat emulsion. Int J Pharm 1986;29: 233–236.
2. Loff S, Kabs F, Witt K, Sartoris J, Mandl B, Niessen KH, Waag KL. Polyvinylchloride infusion lines expose infants to large amounts of toxic plasticizers. J Pediatr Surg 2000;35:1775–1781.
3. Poon R, Lecavalier P, Mueller R, Valli VE, Procter BG, Chu I. Subchronic oral toxicity of di-n-octyl phthalate and di(2-ethylhexyl)phthalate in the rat. Food Chem Toxicol 1997;35:225–239.
4. Lamb JC, Chapin RE, Teague J, Lawton AD, Reel JR. Reproductive effects of four phthalic acid esters in the mouse. Toxicol Appl Pharmacol 1987;88:255–269.
5. Tyl RW, Price CJ, Marr MC, Kimmel CA. Developmental toxicity evaluation of dietary di(2-ethylhexyl)phthalate in Fischer 344 rats and CD-1 mice. Fundam Appl Toxicol 1988;10:395–412.
6. Richburg JH, Boekelheide K. Mono-(2-ethylhexyl)phthalate rapidly alters both Sertoli cell vimentin filaments and germ cell apoptosis in young rat testes. Toxicol Appl Pharmacol 1996;137:42–50.
7. Lee J, Richburg JH, Shipp EB, Meistrich ML, Boekelheide K. The Fas system, a regulator of testicular germ cell apoptosis, is differentially up-regulated in Sertoli cell versus germ cell injury of the testis. Endocrinology 1999;140:852–858.
8. Richburg JH, Nanex A, Williams LR, Embree ME, Boekelheide K. Sensitivity of testicular germ cells to toxicant-induced apoptosis in gld mice that express a nonfunctional form of Fas ligand. Endocrinology 2000;141:787–793.
9. Lovekamp TN, Davis BJ. Mono-(2-ethylhexyl)phthalate suppresses aromatase transcript levels and estradiol production in cultured rat granulosa cells. Toxicol Appl Pharmacol 2001;172:217–224.
10. Habert R, Muczynski V, Lehraiki A, Lambrot R, Lécureuil C, Levacher C, Coffigny H, Pairault C, Moison D, Frydman R, Rouiller-Fabre V. Adverse effects of endocrine disruptors on the foetal testis development: Focus on the phthalates. Folia Histochem Cytobiol 2009;47:S67–S74.
11. Lambrot R, Muczynski V, Lécureuil C, Angenard G, Coffigny H, Pairault C, Moison D, Frydman R, Habert R, Rouiller-Fabre V. Phthalates impair germ cell development in the human fetal testis in vitro without change in testosterone production. Environ Health Perspect 2009;117:32–37.
12. Reinsberg J, Wegener-Toper P, van der Ven K, van der Ven H, Klingmueller D. Effect of mono-(2-ethylhexyl) phthalate on steroid production of human granulosa cells. Toxicol Appl Pharmacol 2009;239:116–123.
13. Silva MJ, Furr J, Preau JL Jr, Samadar E, Fray LE, Calafat AM. Identification of potential biomarkers of exposure to

di(isononyl)cyclohexane-1,2-dicarboxylate (DINCH), an alternative for phthalate plasticizers. J Expo Sci Environ Epidemiol 2012;22: 201–211.
14. Nair CS, Vidya R, Ashalatha PM. Hexamoll DINCH plasticised PVC containers for the storage of platelets. Asian J Transfus Sci 2011; 5:18–22.
15. Jayakrishnan A, Sunny MC, Rajan MN. Photocrosslinking of azidated poly(vinyl chloride) coated onto plasticized PVC surface – Route to containing plasticizer migration. J Appl Poly Sci 1995;56: 1187–1195.
16. Miyamoto M, Sasakawa S. Effects of plasticizers and plastic bags on granulocyte function during storage. Vox Sang 1987;53:19–22.
17. Krishnan VK, Jayakrishnan A. Radiation grafting of hydrophilic monomers on to plasticized poly(vinyl chloride) sheets II. Migration behaviors of the plasticizer from N-vinyl pyrrolidone grafted sheets. Biomaterials 1991;12:489–492.
18. Ito R, Seshimo F, Haishima Y, Hasegawa C, Isama K, Yagami T, Nakahashi K, Yamazaki H, Inoue K, Yoshimura Y, Saito K, Tsuchiya T, Nakazawa H. Novel approach for reducing migration of di-2-ethylhexyl phthalate from polyvinyl chloride medical device. Int J Pharm 2005;303:104–112.
19. Haishima Y, Seshimo F, Higuchi T, Yamazaki H, Hasegawa C, Izumi S, Makino T, Nakahashi K, Ito R, Inoue K, Yoshimura Y, Saito K, Yagami T, Tsuchiya T, Nakazawa H. Development of a simple method for predicting the levels of di(2-ethylhexyl)phthalate migrated from PVC medical devices into pharmaceutical solutions. Int J Pharm 2005;298:126–142.
20. Haishima Y, Matsuda R, Hayashi Y, Hasegawa C, Yagami T, Tsuchiya T. Risk assessment of di(2-ethylhexyl) phthalate eluted from PVC blood circuits during hemodialysis and pump-oxygenation therapy. Int J Pharm 2004;274:119–129.
21. Hayashi Y, Matsuda R, Haishima Y, Yagami T, Nakamura, A. Validation of HPLC and GC-MS systems for bisphenol-A leached from hemodialyzers on the basis of FUMI theory. J Pharm Biomed Anal 2002;28:421–429.
22. Isama K, Matsuoka A, Haishima Y, Tsuchiya T. Proliferation and differentiation of normal human osteoblasts on dental Au-Ag-Pd casting alloy: Comparison with cytotoxicity to fibroblast L929 and V79 cells. Mater Transact 2002;43:3155–3159.
23. Matsuoka A, Onfelt A, Matsuda Y, Nakaoka R, Haishima Y, Yudasaka M, Iijima S, Tsuchiya T. 2009, Development of an in vitro screening method for safety evaluation of nanomaterials. Bio-Med Mater Eng 2009;19:19–27.
24. Matsuoka A, Sofuni T, Miyata N, Ishidate M Jr. Clastogenicity of 1-nitropyrene, fluorine, and mononitrofluorenes in cultured Chinese hamster cells. Mutat Res 1991;259:103–110.
25. Chen CY. The oxidation of di-(2-Ethylhexyl) phthalate (DEHP) in aqueous solution by UV/H_2O_2 photolysis. Water Air Soil Pollut 2010;209:411–417.
26. Ito R, Miura N, Ushiro M, Kawaguchi M, Nakamura H, Iguchi H, Ogino J, Oishi M, Wakui N, Iwasaki Y, Saito K, Nakazawa H. Effect of gamma-ray irradiation on degradation of di(2-ethylhexyl)phthalate in polyvinyl chloride sheet. Int J Pharm 2009;376:213–218.